Adrenodoxin: Structure, Stability, and Electron Transfer Properties

Asya V. Grinberg,[1] Frank Hannemann,[1] Burkhard Schiffler,[1] Jürgen Müller,[2] Udo Heinemann,[2,3] and Rita Bernhardt[1]*

[1]*Naturwissenschaftlich-Technische Fakultät III, Fachrichtung 8.8 — Biochemie, Universität des Saarlandes, Saarbrücken, Germany*
[2]*Forschungsgruppe Kristallographie, Max-Delbrück-Centrum für Molekulare Medizin, Berlin, Germany*
[3]*Institut für Kristallographie, Freie Universität Berlin, Berlin, Germany*

ABSTRACT **Adrenodoxin is an iron-sulfur protein that belongs to the broad family of the [2Fe-2S]-type ferredoxins found in plants, animals and bacteria. Its primary function as a soluble electron carrier between the NADPH-dependent adrenodoxin reductase and several cytochromes P450 makes it an irreplaceable component of the steroid hormones biosynthesis in the adrenal mitochondria of vertebrates. This review intends to summarize current knowledge about structure, function, and biochemical behavior of this electron transferring protein. We discuss the recently solved first crystal structure of the vertebrate-type ferredoxin, the truncated adrenodoxin Adx(4-108), that offers the unique opportunity for better understanding of the structure-function relationships and stabilization of this protein, as well as of the molecular architecture of [2Fe-2S] ferredoxins in general. The aim of this review is also to discuss molecular requirements for the formation of the electron transfer complex. Essential comparison between bacterial putidaredoxin and mammalian adrenodoxin will be provided. These proteins have similar tertiary structure, but show remarkable specificity for interactions only with their own cognate cytochrome P450. The discussion will be largely centered on the protein-protein recognition and kinetics of adrenodoxin dependent reactions. Proteins 2000;40:590–612.** © 2000 Wiley-Liss, Inc.

Key words: adrenodoxin; ferredoxin; iron-sulfur cluster; cytochrome P450; electron transfer

INTRODUCTION

[2Fe-2S]-Type ferredoxins comprise a family of small iron-sulfur proteins that are widely distributed in bacteria, plants, and animals and participate in a broad variety of electron transfer (ET) reactions. As a rule, the ferredoxins are low molecular mass proteins (6–25 kDa) that are negatively charged at neutral pH and contain iron-sulfur clusters as a redox active group. The [2Fe-2S] ferredoxins of bacterial origin fulfill a variety of different functions, e.g., the most extensively studied putidaredoxin or terpredoxin are components of the hydroxylation systems of camphor and α-terpineol, the carbon sources for the host organisms *Pseudomonas putida* and *Pseudomonas sp.*[1,2] In plant-type [2Fe-2S] ferredoxins, the proteins are involved in the transfer of electrons from photosystem I to $NADP^+$ by means of ferredoxin-reductase in the process of carbon assimilation and serve as electron donors to various cellular proteins, such as nitrate reductase, sulfite reductase, and glutamate synthase.[3] The hydroxylation systems of vertebrates use ferredoxins to carry electrons from ferredoxin-reductase to various membrane-bound cytochromes P450.

The structures of several plant-type ferredoxins (from *Anabaena 7120*,[4,5] *Spirulina platensis,*[6] *Aphanothece sacrum,*[7] *Spinacia oleracea,*[8] *Equisetum arvense,*[9] etc.) have been known for a long time and different aspects of electron transfer in these systems have been extensively investigated.[10–15] A recent excellent review of Holden and co-workers[16] provides a throughout discussion on the structure-functional relationship for *Anabaena* ferredoxin and other plant-type ferredoxins. The main goal of the present work is to summarize the information gained in the past decade on a representative of vertebrate-type [2Fe-2S] ferredoxins, adrenodoxin. Previous investigations of our laboratory and others have focused on the electron transfer reaction between adrenodoxin and its redox partners, adrenodoxin reductase and steroid hydroxylating cytochromes P450. The individual proteins in this system are well-characterized biochemically and biophysically. Bovine adrenodoxin has been cloned, overexpressed

Abbreviations: Adx, adrenodoxin; Fdx, ferredoxin; Pdx, putidaredoxin; AdR, adrenodoxin reductase; CYP11A1, cytochrome P450scc; CYP11B1, cytochrome P45011β; WT-Adx, wild-type adrenodoxin; pAdx, preadrenodoxin; Adx(4-108) etc., truncated adrenodoxin comprising residues 4-108 etc.; Adx(4-108A) etc., Adx(4-108) with alanine or another amino acid in position 108; DSC, differential scanning calorimetry; CD, circular dichroism; ET, electron transfer; $\Delta_d G$, Gibbs energy of denaturation.

Grant sponsor: Deutsche Forschungsgemein-schaft; Grant numbers: Be 1343/1-3, Be 1343/8-2, and He 1318/19-1; Grant sponsor: Fonds der Chemischen Industrie.

Dr. Grinberg's present address is Howard Hughes Medical Institute, University of Michigan Medical Center, Ann Arbor, MI 48109.

*Correspondence to: Rita Bernhardt, Naturwissenschaftlich Technische Fakultät III, Fachrichtung 8.8 – Biochemie, Universität des Saarlandes, P.O. Box 15 11 50, D-66041 Saarbrücken, Germany. E-mail: ritabern@rz.uni-sb.de

Received 9 September 1999; Accepted 30 March 2000

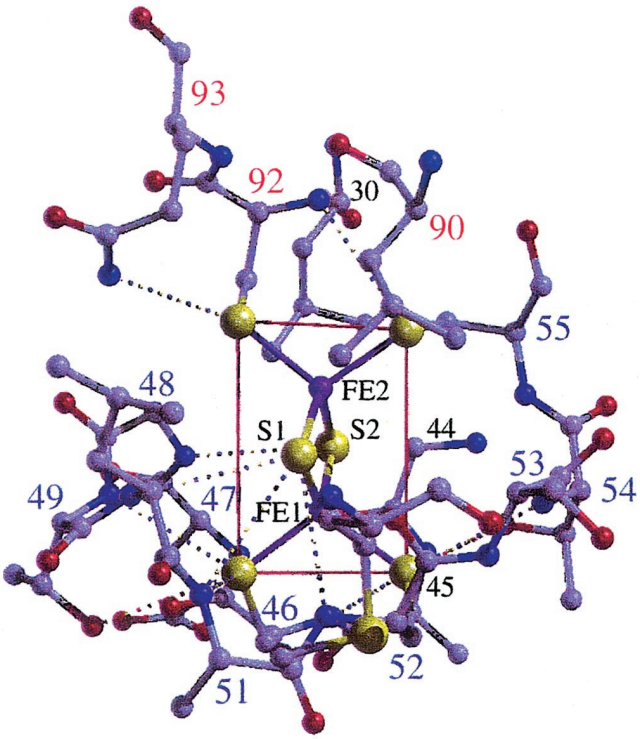

Fig. 1. Region of Adx(4-108) surrounding the iron-sulfur cluster. The Sγ atoms of the [2Fe-2S] cluster-binding cysteinyls 46, 52, 55, and 92 define a plane marked by red lines. Atoms are drawn in ball-and-stick representation; and hydrogen bonds are indicated by dotted lines. Blue numbers label residues included in adrenodoxin motif 1, and red numbers label residues in motif 3 as defined in PROSITE.[39]

in *Escherichia coli*, and the 3-dimensional structure of a truncated Adx(4-108) has been solved recently in our laboratory with high resolution (1.85 Å), thereby making it a perfect candidate for structure-functional studies in this important class of redox proteins. Moreover, when this review was in preparation, Waterman's group reported the crystallization of the full-length adrenodoxin[17] and the crystal structure of adrenodoxin reductase became available.[18] Very recently, we published a comparison of the crystal structures and electron transfer pathways in the vertebrate-type and plant-type ferredoxins.[19]

Adrenodoxin (Adx) supplies electrons from a NADPH-dependent Adx-reductase (AdR) to cytochrome P450scc (CYP11A1), which in adrenals catalyses the side-chain cleavage of cholesterol, and to cytochromes of the CYP11B family, being involved in the formation of cortisol and aldosterone.[20] Adrenodoxin mRNA, which is encoded by a nuclear gene, is translated in the cytoplasm as a higher molecular weight preprotein. It is processed upon import into mitochondria by an endoproteolytic cleavage, which removes the N-terminal amphiphilic presequence (58 amino acids).[21] Mature Adx consists of 128 amino acid residues and has a molecular weight of 14.4 kDa. Little is known about the folding of Adx or other ferredoxins or the mechanism of cluster incorporation. The structure of the [2Fe-2S] cluster of Adx is depicted in Figure 1. Each iron is in tetrahedral coordination with two acid labile sulfurs and two cysteinyl sulfurs (residues 46, 52, 55, and 92). Although the possibility of partial noncysteinyl ligand coordination has been demonstrated for other iron-sulfur proteins[11,22–26] and cysteine-to-serine mutants of some [2Fe-2S] ferredoxins are competent in the electron transfer,[27–29] none of the cysteine ligands in Adx could be replaced with serine residues without destruction of the [2Fe-2S] cluster upon expression in *Escherichia coli*.[30] Whether it will be possible to assemble the cluster into Adx under in vitro reconstitution conditions, as has been performed in the case of other ferredoxins, remains to be elucidated. The oxidized state of the cluster can be sensitively described by absorption spectroscopy, where it shows positive maxima at 320, 414, and 455 nm, or by circular dichroism (CD) spectroscopy.[31] Resonance Raman effect has emerged as a sensitive structural probe for the oxidized [2Fe-2S] clusters and reliable vibrational assignments based on extensive IR and Raman studies are available.[32,33] The reduced state of the iron-sulfur cluster is well characterized by EPR spectroscopy, where it is described by two principal g factors of 1.94 and 2.03, and by Mössbauer spectroscopy.[34,35] By using ^{1}H-NMR spectroscopy, the assignments of the resonances of aromatic amino acids in the oxidized and reduced forms of Adx have been obtained.[36,37]

In this review, we will provide important results of a structural comparison of adrenodoxin and other [2Fe-2S] ferredoxins of the vertebrate- and bacterial-type. Moreover, we describe over 30 mutants of adrenodoxin that have been designed to explore questions about cluster assembly and stabilization and to determine which residues are important for recognition and electron transfer to the redox partners, adrenodoxin reductase, CYP11A1, and CYP11B1.

STRUCTURE OF ADRENODOXIN

Sequence Homology and Folding Pattern

Based on the amino acid sequence relationships, the arrangement of the conserved cysteine residues and geometry of the [2Fe-2S] cluster three rather distant classes can be distinguished among more than 100 known [2Fe-2S] ferredoxins: plant-type, bacterial-type, and vertebrate-type ferredoxins.[38] The proteins inside each group are well conserved. However, the homology between ferredoxins from different groups is rather low (Fig. 2). Thus, the sequence identity between the plant-type and vertebrate-type ferredoxins is less than 23%. The structure in the core region of all ferredoxins is, however, very similar, whereas the region homologous to the so-called "interaction domain" of Adx differs among the adrenal ferredoxin and plant-type ferredoxins.[19] Interestingly, His56, which was shown to play an essential role in connecting the core and interaction domains of Adx (see below), is absolutely conserved in vertebrate-type ferredoxins, but not found in plant-type ferredoxins. In contrast, a hydroxyl group (either serine or threonine) seems to be pivotal in the position homologous to Thr54 of Adx. As shown in Figure 2, the loop between the ligands homologous to Cys46 and Cys55 of

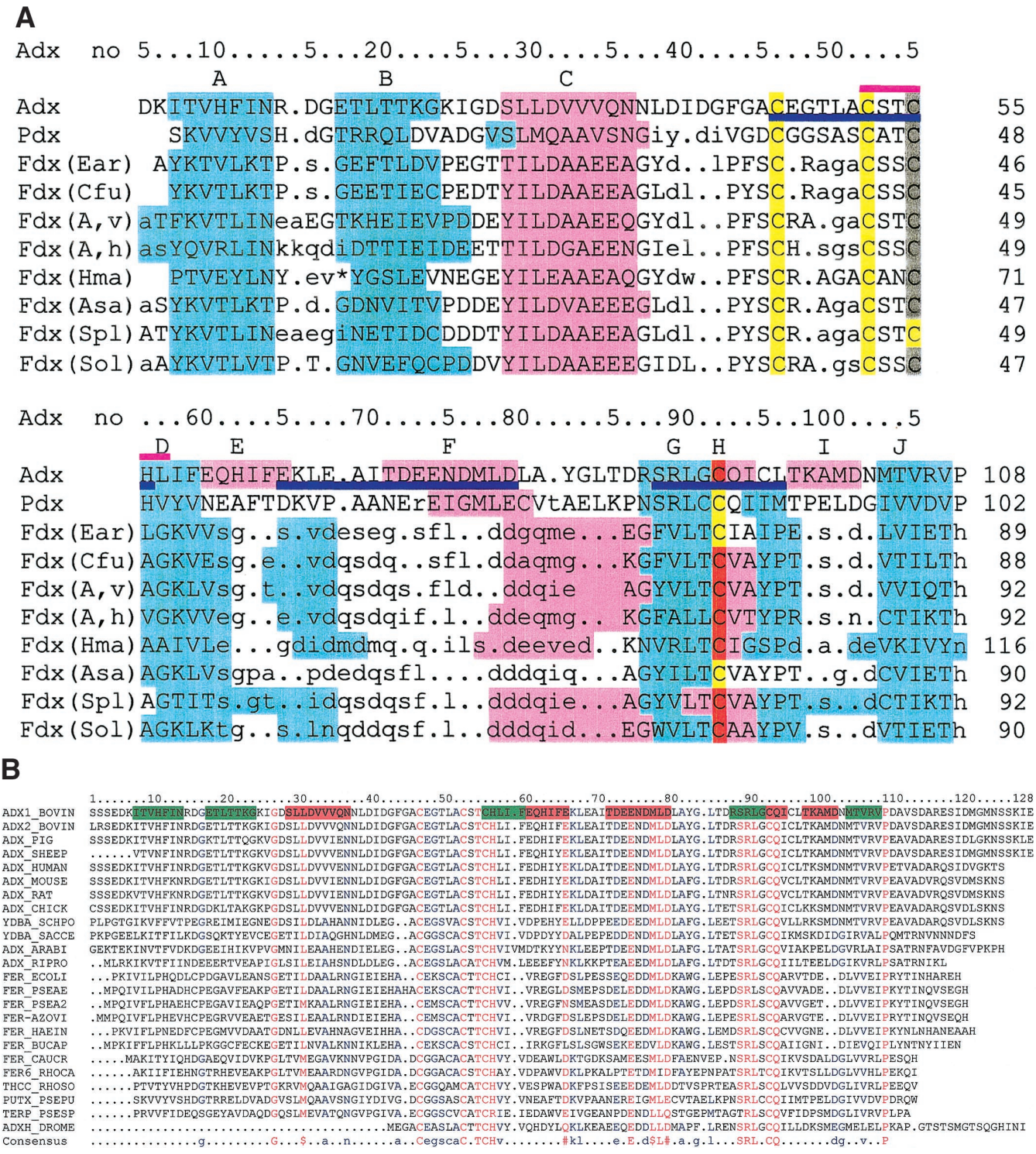

B

```
                 1.......10........20........30........40........50........60........70........80........90.......100.......110.......120.....128
ADX1_BOVIN       SSSEDKITVHFINRDGETLTTKGKIGDSLLDVVVQNNLDIDGFGACEGTLACSTCHLI.FEQHIFEKLEAITDEENDMLDLAYG.LTDRSRLGCQICLTKAMDNMTVRVPDAVSDARESIDMGMNSSKIE
ADX2_BOVIN       LRSEDKITVHFINRDGETLTTKGKIGDSLLDVVVQNNLDIDGFGACEGTLACSTCHLI.FEQHIFEKLEAITDEENDMLDLAYG.LTDRSRLGCQICLTKAMDNMTVRVPDAVSDARESIDMGMNSSKIE
ADX_PIG          SSSEDKITVHFINRDGKTLTTQGKVGDSLLDVVIENNLDIDGFGACEGTLACSTCHLI.FEDHIFEKLEAITDEENDMLDLAYG.LTDRSRLGCQICLTKAMDNMTVRVPEAVADARESIDLGKNSSKLE
ADX_SHEEP        ......VTVNFINRDGETLTTKGKVGDSLLDVVVENNLDIDGFGACEGTLACSTCHLI.FEQHIYEKLEAITDEENDMLDLAYG.LTDRSRLGCQICLTKAMDNMTVRVPDAVSDARESIDMGMNSSKIE
ADX_HUMAN        SSSEDKITVHFINRDGETLTTKGKVGDSLLDVVVENNLDIDGFGACEGTLACSTCHLI.FEDHIYEKLDAITDEENDMLDLAYG.LTDRSRLGCQICLTKSMDNMTVRVPETVADARQSIDVGKTS
ADX_MOUSE        SSSEDKITVHFKNRDGETLTTKGKIGDSLLDVVIENNLDIDGFGACEGTLACSTCHLI.FEDHIYEKLDAITDEENDMLDLAFG.LTDRSRLGCQVCLTKAMDNMTVRVPEAVADVRQSVDMSKNS
ADX_RAT          SSSEDKVTVHFKNRDGETLTTKGKVGDSLLDVVIENNLDIDGFGACEGTLACSTCHLI.FEDHIYEKLDAITDEENDMLDLAFG.LTNRSRLGCQVCLTKAMDNMTVRVPEAVADVRQSVDMSKNS
ADX_CHICK        CSSEDKITVHFINRDGDKLTAKGKPGDSLLDVVVENNLDIDGFGACEGTLACSTCHLI.FEDHIFEKLDAITDEEMDMLDLAYG.LTETSRLGCQICLKKSMDNMTVRVPEAVADARQSVDLSKNS
YDBA_SCHPO       PLPGTGIKVFFVTPEGREIMIEGNEGDSILDLAHANNIDLEG..ACEGSVACSTCHVI.VDPEHYELLDPPEEDEEDMLDLAFG.LEETSRLGCQVLLRKSMDNMTVRVPEAVADARQSVDLSKNS
YDBA_SACCE       PKPGEELKITFILKDGSQKTYEVCEGETILDIAQGHNLDMEG..ACGGSCACSTCHVI.VDPDYYDALPEPEDDENDMLDLAYG.LTETSRLGCQIKMSKDIDGIRVALPQMTRNVNNNDFS
ADX_ARABI        GEKTEKINVTFVDKDGEEIHIKVPVGMNILEAAHENDIELEG..ACEGSLACSTCHVIVMDTKYYNKLEEPTDEENDMLDLAFG.LTATSRLGCQVIAKPELDGVRLAIPSATRNFAVDGFVPKPH
ADX_RIPRO        ..MLRKIKVTFIINDEEERTVEAPIGLSILEIAHSNDLDLEG..ACEGSLACATCHVM.LEEEFYNKLKKPTEAEEDMLDLAFG.LTDTSRLGCQIILTEELDGIKVRLPSATRNIKL
FER_ECOLI        ...PKIVILPHQDLCPDGAVLEANSGETILDAALRNGIEIEHA..CEKSCACTTCHCI..VREGFDSLPESSEQEDDMLDKAWG.LEPESRLSCQARVTDE..DLVVEIPRYTINHAREH
FER_PSEAE        ..MPQIVILPHADHCPEGAVFEAKPGETILDAALRNGIEIEHAHACEKSCACTTCHVI..VREGLDSMEPSDELEDDMLDKAWG.LEPDSRLSCQAVVADE..DLVVEIPKYTINQVSEGH
FER_PSEA2        ..MPQIVFLPHAEHCPEGAVIEAQPGETIMKAALRNGIEIEHA..CEMSCACTTCHVV..VREGFNSMEASDELEDDMLDKAWG.LEPDSRLSCQAVVGET..DLVVEIPKYTINQVSEGH
FER-AZOVI        .MMPQIVFLPHEVHCPEGRVVEAETGESILEAALRNDIEIEHA..CEMSCACTTCHVI..VRDGFDSLEPSDELEDDMLDKAWG.LEPESRLSCQARVGTE..DLVVEIPRYTINQVSEQH
FER_HAEIN        ...PKVIFLPNEDFCPEGMVVDAATGDNLLEVAHNAGVEIHHA..CDGSCACTTCHVI..VREGFDSLNETSDQEEDMLDKAWG.LEMDSRLSCQCVVGNE..DLVVEIPKYNLNHANEAAH
FER_BUCAP        ..MPKIFFLPHKLLLPKGGCFECKEGETILNVALKNNIKLEHA..CEKSCACSTCHCI..IRKGFLSLSGWSEKEEDVLDKAWG.LESTSRLSCQAIIGNI..DIEVQIPLYNTNYIIEN
FER_CAUCR        .....MAKITYIQHDGAEQVIDVKPGLTVMEGAVKNNVPGIDA.DCGGACACATCHVY.VDEAWLDKTGDKSAMEESMLDFAENVEP.NSRLSCQIKVSDALDGLVVRLPESQH
FER6_RHOCA       ......AKIIFIEHNGTRHEVEAKPGLTVMEAARDNGVPGIDA.DCGGACACSTCHAY.VDPAWVDKLPKALPTETDMIDFAYEPNPATSRLTCQIKVTSLLDGLVVHLPEKQI
THCC_RHOSO       ......PTVTYVHPDGTKHEVEVPTGKRVMQAAIGAGIDGIVA.ECGGQAMCATCHVY.VESPWADKFPSISEEEDEMLDDTVSPRTEASRLSCQLVVSDDVDGLIVRLPEEQV
PUTX_PSEPU       ......SKVVYVSHDGTRRELDVADGVSLMQAAVSNGIYDIVG.DCGGSASCATCHVY.VNEAFTDKVPAANEREIGMLECVTAELKPNSRLCCQIIMTPELDGIVVDVPDRQW
TERP_PSESP       ......PRVVFIDEQSGEYAVDAQDGQSLMEVATQNGVPGIVA.ECGGSCVCATCRIE.IEDAWVEIVGEANPDENDLLQSTGEPMTAGTRLSCQVFIDPSMDGLIVRVPLPA
ADXH_DROME       ..........................................MEGACEASLACTTCHVY.VQHDYLQKLKEAEEQEDDLLDMAPF.LRENSRLGCQILLDKSMEGMELELPKAP.GTSTSMGTSQGHINI
Consensus        ..............g.........G...$..a..n......a..CegscaC.TCHv........#kl....e.E.d$L#.a.g.l...SRL.CQ.......dg..v..P
```

Fig. 2. **A:** Structure-based alignment of vertebrate-type and plant-type ferredoxins. Residues at equivalent positions to adrenodoxin are represented by upper-case letters. Helical regions are red, β-strands green, and cluster-liganding cysteinyls yellow (appearing orange in helices, olive in sheets). The residues of Adx are marked with blue bars belong to the adrenodoxin-specific motif, and the peptide strand marked magenta binds specifically to cytochrome c (defined in PROSITE.[39] Adx, adrenodoxin[40]; Pdx, putidaredoxin[51]; Fdx(Ear), ferredoxin from *Equisetum arvense*[9]; Fdx(Cfu), Fdx from *Chlorella fusca*[49]; Fdx(A,v), Fdx from *Anabaena*, vegetative form[4]; Fdx(A,h), Fdx from *Anabaena*, heterocyst form[5]; Fdx(Hma), Fdx from *Haloarcula marismortui*[46]; Fdx(Asa), Fdx from *Aphanothece sacrum*[7]; Fdx(Spl), Fdx from *Spirulina platensis*[6]; Fdx(Sol), Fdx from *Spinacia oleracea*.[8] **B:** Sequence alignment of vertebrate-type [2Fe-2S] ferredoxins that contain the adrenodoxin motif C-x(2)-[STAQ]-x-[STAMV]-C-[STA]-T-C-[HR] (PS00814, PROSITE database.[39] Database searches (GeneStream; http://wwwz.igh.cnrs.fr/) were done with FASTA,[145] and the sequence alignment results are from MultAlin.[146] Consensus levels: high (colored red) ≥ 90%, intermediate (colored blue) ≥ 50%, low (colored gray) ≤ 50% residue identity. $ stands for L or M, # stands for N, D, Q, or E. Helical regions in Adx(4-108) are marked by a red background, β-strands in green. The abbreviations used for ferredoxins are self-explanatory for ADX1_BOVIN, ADX2_BOVIN, ADX-_PIG, ADX_SHEEP, ADX_HUMAN, ADX_MOUSE, ADX_RAT, ADX-_CHICK; YDBA_SCHPO *Schizosaccharomyces pombe*, YDBA_SACCE *Saccharomyces cerevisiae*, ADX_ARABI *Arabidopsis thaliana,* ADX_RIPRO *Rickettsia prowazekii,* FER_ECOLI *E. coli*, FER_PSEAE *Pseudomonas aeruginosa*, FER_PSEA2 *Pseudomonas aeruginosa*, FER_AZOVI *Azotobacter vinelandii*, FER_HAEIN *Haemophilus influenzae*, FER_BUCAP *Buchnera aphidicola*, FER_CAUCR *Caulobacter crescentus*, FER6_RHOCA *Rhodobacter capsulatus*, THCC_RHOSO *Rhodococcus sp* (rhodocoxin), PUTX_PSEPU *Pseudomonas putida* (putidaredoxin), TERP_PSESP *Pseudomonas sp.* (terpredoxin), ADXH-_DROME *Drosophila melanogaster*.

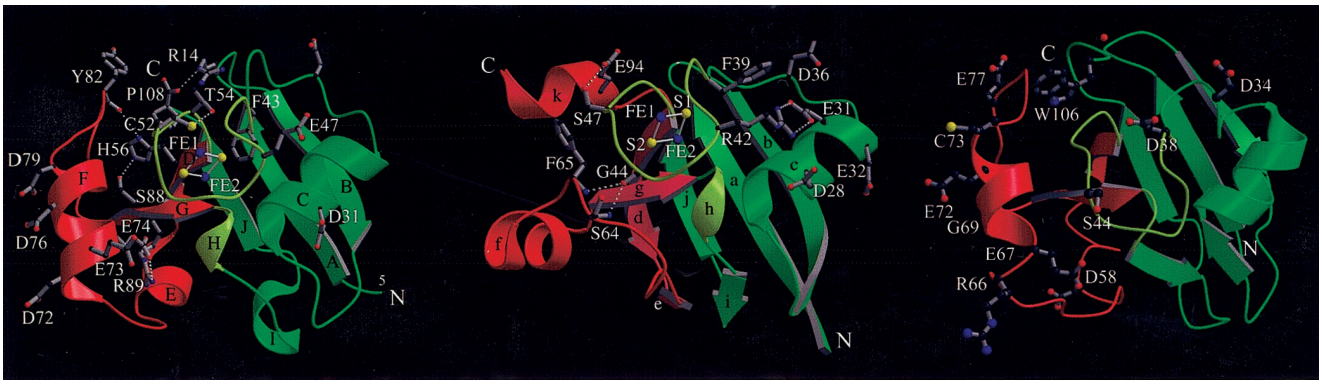

Fig. 3. Ribbon drawing of bovine adrenodoxin Adx(4-108) (left), ferredoxin from *Anabaena* vegetative (middle),[5] and putidaredoxin (right).[41] The interaction domain is colored red, the core domain green, and the iron-sulfur cluster-surrounding region yellow. The [2Fe-2S] cluster is drawn in ball-and-stick representation (Fe, purple; S, yellow). Several hydrogen bonds (dotted lines) and some functionally important residues discussed in the text are included. α-Helices and β-sheets are labeled sequentially by upper case letters (adrenodoxin) and lower case letters (plant-type ferredoxins) as in the sequence alignment in Figure 2A.

Adx is one amino acid shorter in plant-type ferredoxins than that of Adx and Pdx.

At the same time, the proteins within the vertebrate family evidently are highly homologous. The Adx-motif is a three-element fingerprint that provides a signature for the ferredoxins of the hydroxylase-type (PROSITE[39]). The fingerprint was derived from an alignment of 24 sequences: motif 1 includes the region with the three conserved cysteines, which are ligands of the [2Fe-2S] center (residues Cys46-His56); motif 2 contains a cluster of negatively charged residues (Glu65-Asp79), which is essential for binding both the reductase and cytochromes P450; and motif 3 includes the sequence around the fourth conserved Cys ligand of the [2Fe-2S] cluster (Ser88-Gln93) (Fig. 2). These motifs are highly conserved in hydroxylase-type ferredoxins, but alignment of vertebrate-type ferredoxins, resulting from a FASTA database search for proteins, which contain the adrenodoxin motif C-x(2)-[STAQ]-x-[STAMV]-C-[STA]-T-C-[HR], also contains proteins of so far unknown function (Fig. 2B). Moreover, Gly26 and Pro108 are absolutely conserved in all hydroxylase-type ferredoxins known so far. Pro108 was shown to play an essential role in Adx in holding together the C- and N-terminal regions of the protein (see the Conformational Stability and Folding section of this review). It seems conceivable that the corresponding proline residues in the other vertebrate-type ferredoxins have a similar function in stabilizing the respective proteins. The role of Gly26 and the corresponding glycine residues in other ferredoxins has not been investigated so far.

Until now, the structures of only three representative hydroxylase-type ferredoxins, bovine Adx (X-ray structures), bacterial putidaredoxin from *Pseudomonas putida* (NMR), and bacterial terpredoxin (Tdx) from *Pseudomonas sp* (NMR) are known. The sequence identity between Adx and Pdx is 33% in a 101 amino acid overlap (54% similarity), that between Adx and Tdx is 26% (43% similarity). Their structures were compared very recently.[40–42] The structural alignment shows that the secondary and tertiary structures are much higher conserved than the primary structures. The lately obtained X-ray data on the truncated Adx(4-108)[40] provide the first description of a vertebrate ferredoxin and serve to explain a large body of biochemical studies in terms of a 3-dimensional structure. The protein displays the compact (α + β) fold typical for [2Fe-2S] ferredoxins. Approximately 27% β-strand, 23% α-helix, and 7.5% 3_{10} helix has been recognized. Five β-strands and five helices were identified and are here assigned by capital letters beginning from the N-terminus: β-strands *A* (Ile7-Asn13), *B* (Glu17-Gly23), *D* (Cys55-Phe59), *G* (Ser88-Gly91), *J* (Met103-Val107) belong to one β-sheet of mixed type (Fig. 3). *G* and *D*, *D* and *J*, *A*, and *B* are paired in antiparallel orientation, *J* and *A* are parallel. Three of the helices, *C* (Ser28-Asn36), *E* (Glu60-Glu65), and *F* (Thr71-Asp79), are α-helixes, and both *H* (Gly91-Gln94) and *I* (Lys98-Met100) are of the 3_{10}-helix type. The crystallized truncated Adx(4-108) ends with the residue Pro108, whereas the wild-type protein is 128 amino acids long.[19] NMR data have proposed this hydrophilic C-terminal region to rotate freely in solvent and failed to provide evidence of secondary structure elements in this region.[43] While this review was in evaluation, Pikuleva and co-workers solved the full-length structure of bovine adrenodoxin at 2.5 Å resolution by means of molecular replacement by using the structure of the truncated Adx(4-108) as a starting model.[17] Comparison of the structures of full-length and truncated Adx(4-108) revealed that residues 109-111 form a loop directed out into the solvent, whereas no electron density for the rest of the C-terminal part of the molecule (residues 112-128) has been observed. The latter fact indicates once more that this region is highly flexible and free to move in the solution. Interestingly, the ability of full-length Adx to form dimers both in crystalline state and in solution raises the question about its physiologic significance.

The solution structure of the related ferredoxin from *Pseudomonas putida* has been solved by a combination of NMR and computer modeling of the [2Fe-2S] cluster region.[41,44] The superposition of the structures of Adx and Pdx has shown that the main difference among secondary

structure elements is the lack in Pdx of the 3_{10} helices *H* and *I* and of the C-terminus of Adx. Instead, in Pdx the corresponding part is composed of a β-strand (88-90) and a β-turn. Regions with the largest geometric deviation between the two structures involve the sequences Asn36-Gly42 (average distance 4.0 Å for Cα atoms) preceding the cluster binding loop Phe43-Thr54; the N-terminus, especially Asp15 (5.0 Å for Cα atoms); and the β-turns at Asp80-Arg88 (1.9 Å for Cα atoms) just after the deletion between Asp79 and Leu80. The latter region is located at the end of the acidic binding region and includes Tyr82 (Ala in Pdx) known to be important in the recognition of cytochromes P450. Both regions show poor secondary structure.[40] Recently, Mo et al.[42] solved the solution structure of the bacterial oxidized terpredoxin from *Pseudomonas sp*. All three structures are very similar, especially the hydrophobic core domains. An overall RMSD (root mean square deviation) of 2.6 Å for Cα atoms has been determined between Adx, Pdx (model 10 of databank entry 1put[45]), and Tdx (model 3 of entry 1b9r), regardless of crystal or solution structure.

Three-dimensional structures of several plant-type ferredoxins, including proteins from *Aphanothece sacrum*,[7] *Anabaena*,[4,5] *Equisetum arvense*,[9] *Haloarcula marismortui*,[46] *Spirulina platensis*,[6] *Spinacia poleracea*,[8] *Synechococcus elongatus*,[47,48] and *Chlorella fusca*[49] have been known for some time. These ferredoxins have essentially the same fold, each containing a sheet that consists of four major β-strands and one major α-helix flanking the sheet. This motif, called β-grasp motif,[50] is found also in Adx, Pdx, and Tdx. Thus, we can summarize that plant-, bacterial-, and vertebrate-type ferredoxins share the general main-chain fold. A detailed structural comparison and computations of the electron pathways in both vertebrate and plant ferredoxins has been published very recently.[19]

The polypeptide chain of Adx is organized into a large core domain, which contains the [2Fe-2S] cluster and an interaction (recognition) domain, which includes residues previously determined to be involved in interactions with both redox partners, AdR and CYP11A1 (Fig. 3). Residues Asp5-Cys55 and Gly91-Pro108 belong to the core domain, residues 56-90 form a large hairpin bearing the key residues for recognition of AdR and CYP11A1. It comprises the two α-helices *E* and *F*, the loops 64-79 and 80-88, consisting of β-turns 81-84 and 85-88 and β-strands *D* and *H*. The interaction domain is more flexible than the core domain.[40] This conformational flexibility may be relevant for the interaction with reductase and cytochromes. The domains are connected by a limited number of intramolecular interactions allowing for some domain motion. In summary, the core domain, active in the ET processes is much more conserved compared with the region participating in the protein-protein recognition with the diversity of redox partners.

Charged residues of Adx(4-108) are clustered to yield a strikingly asymmetric electric potential of the protein molecule (Fig. 4). There is a drastic segregation of surface charges rendering one face of Adx almost completely acidic. It seems likely that the clearly asymmetric charge distribution at the surface of Adx(4-108) is involved in electrostatic steering of the interactions with AdR and CYP450. Possibly, the strongly inhomogeneous electric field controls the path for the Adx interaction domain to AdR and CYP11A1 or CYP11B1 before any tight molecular docking occurs. This assumption is supported by the asymmetric charge distribution observed for CYP101, a homolog of CYP11A1.[51]

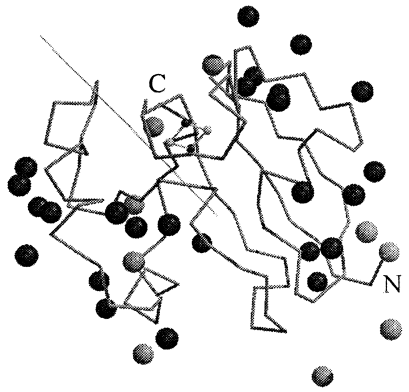

Fig. 4. Cα trace of Adx(4-108) and charge distribution. Negative charges are represented by dark gray spheres (at positions of $O^{\delta 1}$ and $O^{\epsilon 1}$ atoms of aspartate and glutamate residues) and positive charges by light gray spheres (at positions of N^{ϵ} and N^{η}atoms of arginine and lysine residues). The position of the dipole moment vector as calculated with GRASP[147] is indicated by a straight line.

Environment of the Iron-Sulfur Cluster and Redox Potential

The binding region around the [2Fe-2S] cluster (loops Phe43-Cys55, Cys92-Ile94) of Adx is situated in a protrusion of the protein and is protected from direct solvent contact by the cluster-binding segment Leu30, Phe43-Thr54, Met77, Cys92, Gln93, Ile94, and by the hydrophobic core, which includes side chains from residues Cys55, Leu50, Met77, Leu78, Leu90. The X-ray structure of Adx yields the first structural information about the geometry and fine features of the hydroxylase type [2Fe-2S] cluster, because the NMR-deduced structure of Pdx does not give the fine structure of the cluster because of the paramagnetic broadening of the NMR signals by the cluster. In Adx, the [2Fe-2S] cluster is attached to the protein by Fe-Sγ bonds at cysteine residues 46, 52, 55, 92 (Fig. 1). Both the inorganic sulfur atoms in the cluster and the four cluster-Sγ-binding atoms from the protein moiety are involved in an asymmetric network of H-bonds (Table I). Fe_1 seems to be favored over Fe_2 for ET. In general, it is nearer to the surface[40,52,53] and has a much more polar surrounding than Fe_2.[54] Moreover, Fe_1 has been identified to be more reducible by measuring the Nuclear Overhauser effect.[52]

Replacement of any of the cysteine ligand residues in adrenodoxin (cysteines 46, 52, 55 and 92) with serine lead to the formation of an apoprotein when the mutant was expressed in *E. coli*.[30] Whether the iron-sulfur cluster can be assembled in the mutants by using in vitro reconstitu-

TABLE I. Potential Hydrogen Bonds Around the [2Fe-2S] Cluster in Adrenodoxin

Acceptor (A)		Donor (D)		Distance (D–A)
[2Fe-2S] cluster	S1	Glu47	N	3.6[a]
[2Fe-2S] cluster	S2	Cys52	N	3.6[a]
Cys46	Sγ	Gly48	N	3.4*[b]
Cys46	Sγ	Ala51	N	3.3[b]
Cys52	Sγ	Thr54	N	3.4[b]
Cys52	Sγ	Cys46	N	3.7[a]
Cys52	Sγ	Thr54	Oγ1	3.2[b]
Cys55	Sγ	Cys92	N	3.6**
Cys92	Sγ	Gln93	Nϵ2	3.3*

[a]H-bonding criterion according to Fukuyama et al.[143] N-S-N distance < 3.7Å, < 60° deviation from the straight line.
[b]H-bonding criterion according to Stout et al.[142] N-S-N distance < 3.5Å, < 40 deviation from the straight line.

tion has to be elucidated. The [2Fe-2S] clusters of the ferredoxins from *Clostridium pasterianum*,[28] *Anabaena* vegetative,[29] and human placenta,[27] or the [2Fe-2S] center of *E. coli* fumarate reductase[26] can be reconstituted, when the cysteine cluster ligands are replaced by serine and in the case of fumarate reductase also by aspartic acid. The polypeptide chain around the coordinating cysteine residues is rather conserved within the family of the [2Fe-2S]-type ferredoxins, whereby the plant-type ferredoxins display a higher degree of overall sequence similarity than the vertebrate-type ferredoxins (Fig. 2). This is a possible reason for the essential differences in spectrochemical and redox properties among ferredoxins of different types. The variations in band intensities and energies in CD and Resonance Raman spectra and in the values of the principal *g* factors of the EPR spectra of the proteins from plant and animal origin are clearly evident.[32,55] Additionally, despite the common [2Fe-2S] geometric pattern, the ferredoxins cover a wide range of reduction potentials. Hence, redox potentials of plant ferredoxins are mostly lower (from −325 to −425 mV) than those for vertebrate ferredoxins (from −235 to −273 mV).[10,56]

The electron transfer (ET) in biological systems is performed by cascades of different redox partners containing redox-active metals. Their redox potential is a measure for the thermodynamic probability of ET because the redox potential difference is the driving force for electron transfer between reactants (i.e., the ability to accept or donate electrons). The free energy of the reaction (ΔG°) is directly related to the difference in reduction potentials of the partners (ΔE°) through the equation: $\Delta G^\circ = -nF\Delta E^\circ$, where n is the number of electrons involved and F is the Faraday constant. It is, thus, of primary interest to precisely assess which features tune the values of reduction potentials in redox metalloproteins as they are of fundamental importance for the function of these proteins. Adx is of particular interest, because it is part of a mitochondrial electron transport chain that activates dioxygen at the expense of NADPH. Its role as a protein ET intermediate is to accept electrons from AdR and donate them to the mitochondrial cytochromes CYP11A1, CYP11B1, and CYP11B2. These ET reactions span a wide

TABLE II. Redox Potential of Adrenodoxin and Mutants[†]

Adx variant	Redox potential (mV)	Reference
WT-Adx	−273	70
Adx(4-128)	−267	70
Adx(4-114)	−342	70
Adx(4-108)	−344	64
Adx(4-107)	−348	64
Adx(4-108A)	−337	65
Adx(4-108S)	−342	65
Adx(4-108K)	−368	65
Adx(4-108W)	−334	65
Adx(4-108)/R14A	−331	68
Adx(4-108)/R14E	−325	68
T54S	−329	56
T54A	−340	56
Y82F	−274	97
Y82L	−274	97
Y82S	−282	97
H56Q	−302	37
H56T	−340	37
H56R	−339	37
D76E	−274	109

[†]Redox potentials were measured by the dye photoreduction method with Safranin T as indicator and mediator. The data were analyzed according to the Nernst equation. The standard deviation for the method was ±5 mV.

range of redox potentials with −320 mV for NADPH at one end of the chain to +800 mV for oxygen at the other end. The factors that could be responsible for the differences in redox potential of proteins, especially between various ferredoxins include (1) the hydrogen bond network in the vicinity of the cluster, especially to the iron ligands,[57,58] (2) cluster solvent exposure,[59] and (3) the charged side chains of residues and their distribution over the molecule,[58] (4) hydrophobicity of metal environment.[60] However, the relative contribution of each of these factors to the redox potential of iron-sulfur proteins remains to be established for most of the cases. Different studies, including site-directed mutagenesis studies, give valuable hints on the role of the factors tuning the redox potential of Adx and related proteins.[56,61,62] The redox potentials of the mutant Adx proteins vary greatly (Table II). Replacements of residues proposed to be involved in the network of hydrogen bonds around the [2Fe-2S] cluster provides essential information about contributions of this network in the control of the redox potential and modulation of the cluster properties in different types of ferredoxins.[56,63] Thr54 of Adx is located between two of the cysteinyl ligands of the cluster and hydrogen bonded with Cys52 Sγ (N Thr54 - Sγ Cys52 [3.42 Å] and Oγ1 Thr54 - Sγ Cys52 [3.17 Å]). In this position, threonine or serine has been conserved in many [2Fe-2S] ferredoxins. Elimination of the hydrogen bond donor, the OH group, in the mutant T54A results in a drop of the redox potential by 66 mV, indicating the importance of this H-bond in redox potential modulation (Table II). On the other hand, replacement of Thr54 by another hydrogen bond donor (Ser) also results in a lowering of redox potential by 55 mV.[56] It is interesting that, although the threonines in this position in Adx and Pdx are in similar

settings, they form different hydrogen bonds to Asp38 Oδ2 in Pdx, and to Cys52 Sγ in Adx. The redox potential of Pdx is −235 mV,[61] which is 40 mV higher than that of Adx (−275 mV).[56]

Correll et al.[63] proposed H-bonding to be a main controlling factor for a higher redox potential of the iron-sulfur cluster in phthalate dioxygenase reductase compared with the potentials of plant-type ferredoxins. However, the X-ray structural data have not supported the hypothesis of a general relationship between cluster protein H-bonds and experimental redox potential.[19,29,40] For example, the truncated Adx, possessing the lower redox potential (−344 mV),[64] has rather weak H-bonds to the iron-sulfur cluster compared with the plant Fdx (Table I[19]). Thus, the importance of the H-bonding events in the immediate surrounding of the [2Fe-2S] cluster seems to be limited with respect to Adx and related ferredoxins.

The molecular electrostatic potential and/or charge distribution could be of greater importance in controlling the redox potential of Adx (Fig. 4). The deletion of 14 and 20 hydrophilic C-terminal amino acids decreases the negative net charge of Adx from −13 to −12 and −9, respectively. However, this does not influence the redox potential in the expected manner (Table II). A tail protecting the iron-sulfur cluster from contact with the solvent and contributing to the charge surrounding the cluster by its negative net charge would be expected to increase the redox potential of the truncated mutant, compared with WT-Adx. Because the experimental redox potential value for Adx(4-108) is measured as −344 mV, which is 70 mV lower than for wild-type Adx,[65] the shielding effect of the tail seems to be superior to the charge effect. This finding supports the hypothesis that the C-terminus of the adrenodoxin molecule is highly flexible in solution.

The special charge distribution of Adx results in a large dipole moment Figure 4. Magnitude and direction of the moment may play a biologically relevant role during the docking process of the ferredoxins to the electron donors and acceptors.[19,40] The negative end of the dipole vector of Adx crosses the molecular surface near the residues Asp79, Asp76, Asp72, and Glu73,[19] the residues interacting in human ferredoxin with reductase and cytochrome P450.[67] The vector from Fe_2 to Fe_1 within the [2Fe-2S] cluster points nearly in the same direction, whereby the entrance of the modeled electron pathway[19] lies in direct neighborhood to the dipole moment break-through point. The influence of dipole moment changes on the redox potential and on the docking kinetics should be investigated experimentally by mutations of residues not included in interaction or ET processes but influencing the dipole moment. However, it might also be possible that dipoles do not play a significant role in the docking process, but the partner proteins search each other in a semiclosed sphere and then optimize charge and nonpolar interactions.[66] Elimination of a positive charge at the solvent-exposed position 14 (Adx(4-108)/ R14A mutant), which is far removed from the iron-sulfur center, slightly increased the redox potential by 12 mV (Table II). The charge reversed mutation Arg→Glu, further increased the redox potential to −325 mV, compared with −344 mV for Adx(4-108).[68]

Although the surrounding of the first three cluster ligands in bovine adrenodoxin has been exhaustively studied,[56,69,70] the vicinity of the fourth cluster ligand, Cys 92, has not been considered so far. Cys92 is preceded by a highly conserved ^{88}SRL^{90} motif and followed by a conserved Gln. Interestingly, the side chain of arginine 89 is involved in the formation of the unique salt bridge with glutamate 74 that is supposed to play a role in the interdomain interactions in adrenodoxin.[71] It is also attractive to suggest that the positive charge of Arg89 can play some role in the stabilization of the cluster during the reduction process. As described in the literature, elimination of the positive charge near the cluster would make it harder to reduce the protein, because it lowers the reduction potential. Indeed, mutation of Arg89 to alanine changed the redox potential of adrenodoxin from −272 mV to −306 mV. However, charge independent mutations such as Arg89Lys and Glu74Asp also introduced a negative shift of the redox potential, which complicates the interpretation of the data.[71]

CONFORMATIONAL STABILITY AND FOLDING

Attempts to study the unfolding of ferredoxins failed until recently because of the chemical destruction of the iron-sulfur cluster before the unfolding of polypeptide chain. In the presence of oxygen, solvent denaturation of Adx, Pdx, or spinach Fdx with urea or Gdn-HCl was shown to be an irreversible process.[72–74] Both chemical and enzymatic reconstitution of these proteins could be performed under anaerobic conditions only.[69,75] Thus, the oxygen sensitivity of the iron-sulfur cluster during denaturation seems to be a very important common problem that excluded so far this widely distributed group of proteins from intense studies of their folding process. Without protecting reagent, adrenodoxin becomes an apoprotein upon denaturation, which is an irreversible process with respect to cluster rebuilding. However, introduction of reducing agents such as dithiothreitol (DTT) results in reversibility of the unfolding transition even under aerobic conditions. Upon removal of the denaturant, we observed 65, 63, and 64% refolding of adrenodoxin based on CD, fluorescence, and activity measurements, respectively.[76] Interestingly, no addition of iron and sulfide is necessary for the successful refolding. Moreover, ultrafiltration and gel-filtration-chromatography conclusively demonstrated the metal cluster to be bound to the protein during denaturation in the presence of DTT. In the case of thermal denaturation, the percentage of refolding was approximately 60% according to CD measurements. Recently, Burova et al.[77,78] demonstrated by means of microcalorimetry that the [2Fe-2S] cluster in Adx can be highly stabilized by using a buffer system with Na_2S and 2-mercaptoethanol that prevents its destruction before the thermal transition of the polypeptide chain of Adx. Under these conditions, the polypeptide chain undergoes a reversible folding/unfolding transition without dissociation of the iron-sulfur cluster. This process is almost perfectly

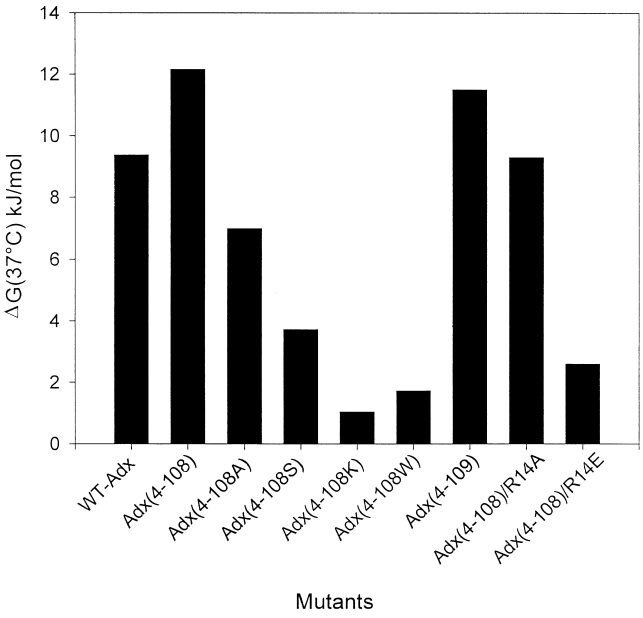

Fig. 5. Effect of mutations on the stability of adrenodoxin. Mathematical treatment of the unfolding curves obtained by CD was made by using a nonlinear regression fit assuming the two-state model of protein denaturation.

described by a two-state model.[79] The differential scanning calorimetry (DSC) and CD data have shown that Adx is a protein of extremely low conformational stability ($\Delta_d G$ approximately 21 kJ/mol at 25°C and pH 8.5),[77] compared with 25–60 kJ/mol for most of globular proteins.[79] To understand whether this marginal stability is favorable in forming ET complexes with various redox partners we studied different mutants of Adx. No simple correlation between conformational stability and functional properties could be found. However, some functionally important residues were identified to play a significant role in stabilizing the Adx structure. Thus, replacement of His56, which supports contacts between the interaction and core domains of the Adx polypeptide chain by Thr, Arg, or Gln reduces the $\Delta_d G$ values by 5.1, 4.9, and 7 kJ/mol, respectively. By contrast, the replacement of the residue participating in the recognition of redox partners, Tyr82, by Leu, Phe, or Ser did not influence significantly thermodynamic parameters. Mutation of the functionally significant Asp76 brought forth even a slight protein stabilization of 1.8 kJ/mol.[78]

Of particular significance for the stability of Adx is the proline residue in position 108, which is highly conserved among vertebrate, many bacterial, yeast, and some plant ferredoxins. Deletion of this residue results in the formation of a misfolded protein that is not able to incorporate the iron-sulfur cluster upon expression in *E. coli*.[80] Replacement of Pro108 by other amino acids, Ala, Lys, Ser, or Trp, does not induce essential functional change.[65] However, the mutations lead to disruptive protein destabilization ($\Delta(\Delta_d G)$ from 5 kJ/mol to 10.7 kJ/mol at 37°C) (Fig. 5). Comparison of the thermodynamic and structural data has shown that Pro108 stabilizes the conformation threefold: (1) through favorable hydrophobic contacts with Ile58, His56, Tyr82; (2) providing the low conformational entropy of unfolding that contributes favorably (5 kJ/mol) to the difference between stabilizing and destabilizing forces upon folding, and finally (3) through important contacts between β strand *J* and the β turn between strands *A* and *B* connected by a hydrogen bond Arg14-Pro108. The elimination of the hydrogen bond between conserved Pro108 and Arg14 costs the protein approximately 6 kJ/mol in terms of stability at physiologic temperature.[68]

Thr54, a residue in the immediate environment of the [2Fe-2S] cluster, was shown to be directly involved in cluster stabilization, participating in H-bonding to the cluster ligand Cys52 Sγ. Elimination of the hydrogen bond donor group (mutant T54A) destabilizes the protein by 5.5 kJ/mol.[78] The mutation on the unique salt bridge Arg89-Glu74 inside the protein core of Adx leads to an extreme protein destabilization and disruption of the interactions between the cluster containing core domain and interaction domain (Fig. 5). Moreover, replacement of glutamate at position 74 by either Ala or Gln in human ferredoxin results in the formation of misfolded apoprotein.[81] The unusual thermal stability of Adx in the alkaline medium (up to pH 10.2) provides a further hint for the importance of the side-chain hydrogen bonds of the lysyl-carboxylate type for the stabilization of the folded conformation of Adx.

Summarizing, we conclude that the internal and external hydrogen bonds and salt bridges seem to play a main role in the stabilization of the Adx structure. This assumption is in line with the prediction of Perutz and Raidt, who compared the structures of [4Fe-4S] ferredoxins from mesophilic and thermophilic organisms and concluded that the greater stability of the latter arises mainly from external salt bridges linking residues near the N-terminus to others near the C-terminus and from additional hydrogen bonds, but apparently not from more nonpolar contacts.[82] Very recently, a 3-dimensional structure of a thermostable [2Fe-2S] ferredoxin from *Synechococcus elongatus* was evaluated by means of 2-dimensional NMR and computer modeling.[47,48] As has been shown for many other proteins from thermophilic and mesophilic organisms, the main-chain structure of the thermostable ferredoxin was almost the same as the crystal structures of other mesophilic ferredoxins. However, comparison of the side-chain structures revealed two unique charge networks in this thermostable Fdx structure, which might contribute to the thermal stability.

The folding mechanism of Adx remains obscure. As has been already mentioned, Adx is synthesized in the cytoplasm as a precursor and is transported into mitochondria with 58 N-terminal amino acids being removed upon the uptake. The targeting sequence of preadrenodoxin (pAdx) could in theory form an independent folding domain. Surprisingly, the presequence does not significantly change the folding pathway of the mature part of the protein, according to the DSC and limited proteolysis data. Moreover, it has a rather minor influence on the stability of the protein.[83] The temperature of denaturation was only slightly reduced compared with that of the mature protein,

although a 50 kJ/mol decrease in the enthalpy of unfolding was observed. The main difference between these two proteins is that a specific residual structure is formed upon thermal unfolding of pAdx as judged from the decreased heat capacity increment value, whereas mature Adx denatures according to the two-state model.[83] Moreover, the unfolded pAdx carries an entrapped iron-sulfur cluster, whereas the mature Adx loses the cluster under the same conditions. Thus, it could be speculated that the newly synthesized pAdx is able to take up and to keep the cluster in a transport-competent structure in a similar manner in the cytoplasm of the mammalian cell. Interestingly, investigations of the role of molecular chaperones in the folding of adrenodoxin suggested that GroEL does not interact specifically with mature adrenodoxin but has a significant effect on the folding rate of the preadrenodoxin.[84] Further studies are necessary to draw a conclusive picture on the role of different chaperons in the folding/refolding process and the cluster assembly of adrenodoxin.

INTERACTION OF ADRENODOXIN WITH ITS REDOX PARTNERS

Models for Electron Transfer by Means of Adrenodoxin

Despite a wealth of information provided from kinetic and thermodynamic studies of the components of steroid hydroxylation systems, the way in which the redox partners interact during electron transfer is still a matter of controversial discussion. Three different mechanisms were proposed for the ferredoxin-mediated ET from AdR to CYP450. A ternary complex of AdR, Adx and $P450_{scc}$ has been observed by Kimura in the presence of cholesterol and phospholipid.[85] Akhrem and coworkers[86] also reported from their chemical modification studies that an organized complex among three proteins is active in the electron transfer reactions of mitochondrial steroid hydroxylase. More recently, optical biosensor studies revealed the formation of a ternary complex between CYP11A1, AdR, and Adx, although competition of CYP11A1 and AdR for the binding with the same or closely placed negatively charged groups on the surface of immobilized Adx was observed.[87] In contrast, Lambeth and co-workers suggested Adx to be a mobile shuttle that initially forms a complex with AdR, dissociates after accepting an electron and finally associates with and transfers a reducing equivalent to the cytochrome P450; the reoxidized iron-sulfur protein then migrates back to the flavoprotein and the cycle is repeated.[88] Elegant rotational diffusion studies of Schwarz and co-workers,[89] by using EPR and ST-EPR, provide a direct evidence that in liposomes binary complexes between Adx and AdR and Adx and CYP11A1 are formed, whereas the existence of a ternary complex can be excluded. An additional clue comes from the 3-dimensional

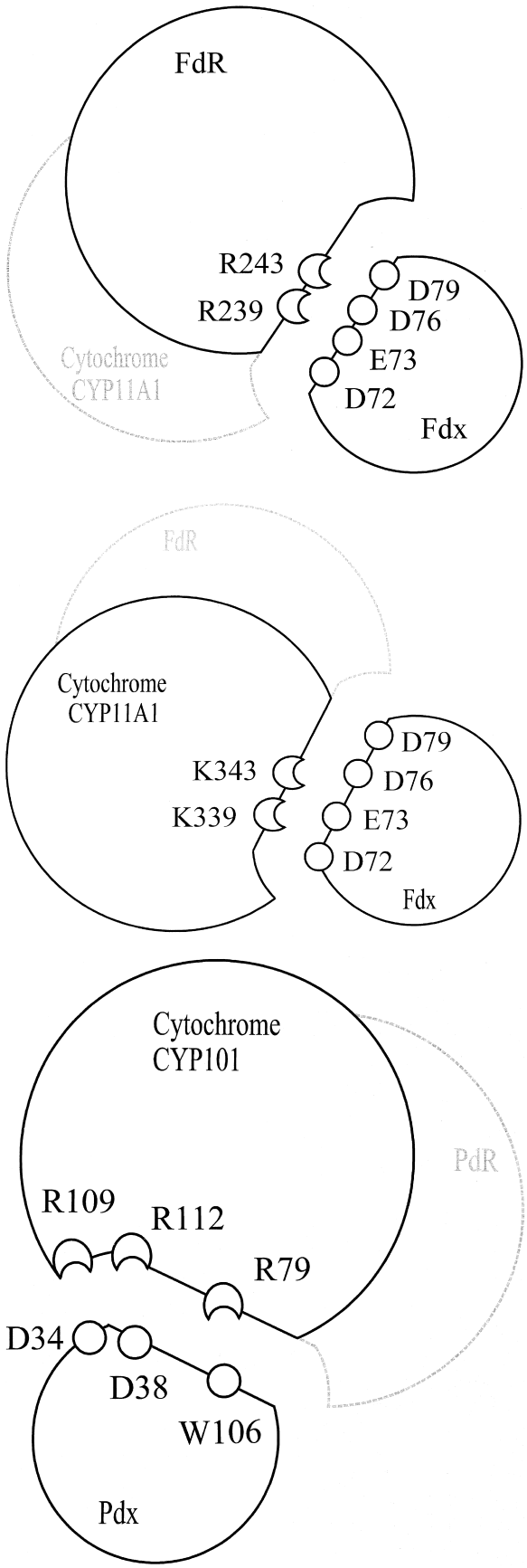

Fig. 6. Schematic representation of protein-protein interactions between Fdx and Pdx and their respective redox partners. Amino acids identified by modification and mutagenesis studies as being involved in binding of the partner molecule are indicated.

structure of AdR, which has been resolved with 2.8 Å resolution.[18] This protein shows a highly asymmetric charge distribution rendering the cleft between the FAD- and the NADPH-domains almost completely basic, whereas the opposite side of the protein is predominantly acidic (Fig. 6). This cleft has been proposed to bind to negatively charged residues of Adx,[18] which have been identified by chemical modification and site-directed mutagenesis studies.[81,90] The review of Vickery[67] gives an excellent synopsis about the residues of Adx, AdR, and CYP11A1 being involved in redox partner interaction. Finally, the necessity of two molecules of Adx for one electron transfer has been proposed in experiments in the natural CYP450 lipid environment (liposomes). This mechanism includes the formation of the quaternary complex consisting of AdR, Adx, and CYP11A1 with a ratio of 1:2:1. The active form is suggested to be a binary-binary transient complex in which Adx is bound to AdR and cytochrome P450, respectively.[91,92] Results of Pikuleva et al.[17] studying the tertiary structure of full-length bovine Adx, suggest the occurrence of functional dimers of Adx supporting such binary-binary, but also ternary (AdR-Adx-Adx, CYP11A1-Adx-Adx) or even quaternary (AdR-Adx-Adx-CYP11A1), electron transfer complexes. Taking into account all these observations, it seems to be possible that under different conditions and with various cytochromes P450, different electron transfer complexes could exist.

Complex Formation Between Adrenodoxin and Adrenodoxin Reductase

General remarks

A prerequisite for the electron transfer between AdR and Adx is the reduction of AdR by NADPH. Chu and Kimura showed that the K_m for the binding of NADPH/NADH to AdR is 1.82 μM and 5.56 mM, respectively, whereas $NADP^+$ inhibits the NADPH-cytochrome *c* reductase activity with a K_i of 5.32 μM. They also demonstrated a 1:1 complex formation between AdR and Adx.[93] Lambeth and Kamin[94] confirmed these results and showed the existence of a two-electron-reduced complex between AdR and $NADP^+$ with a low dissociation constant K_d of 10 nM. By using rapid mixing techniques the reduction of AdR by NADPH yielding a 1:1 complex was demonstrated to be of first order with a k_{app} value of 28 s^{-1}.[70]

The interaction of the wild-type adrenodoxin and its mutants with the electron donating flavoprotein adrenodoxin reductase is measured after cytochrome *c* reduction by the iron-sulfur protein.[88,94,95] The distance between the FAD group of AdR and the cysteine residue 95 (the only free cysteine residue) of Adx was estimated as 36 Å by Förster energy transfer calculations.[96] Although the use of cytochrome *c* as a monitor is a nonphysiologic reaction, it is widely used to investigate the AdR-Adx interaction,[80,81,88,90,97] because the one-electron transfer to Adx seems to be the slowest and thus the rate limiting step in this reaction.[98] Hence, in this assay, the apparent K_m for Adx approximates the K_d of reduced Adx for AdR.

The affinity of AdR for Adx was found to be high ($K_d \sim$ 20–100 nM[99]). However, the association of the two proteins is strongly dependent on the ionic strength indicating that electrostatic interactions are the most important forces for the complex formation.[94,100] Upon reduction of the iron-sulfur center, the K_d value of the AdR-Adx complex is shifted from 25 nM to 540 nM,[88] promoting the dissociation of the reduced Adx from AdR. Despite the tight binding, the *off* rate constant of the oxidized complex was determined to be 300 s^{-1} by using data from time resolved measurements.[101] This *off* rate was shown to be independent on salt concentration, which was varied in a wide range. The calculated *on* rate for the complex formation is given with 180,000 s^{-1}without addition of salt to the used buffer. Very recent optical biosensor studies[87] determined the *off* rate to be 0.02 s^{-1} and the on rate with 18,000 s^{-1}. The discrepancy between these results and the indirect method of monitoring the cytochrome *c* reduction[101] seems to depend on the different methods used. The biochemical method measures the functional complex formation by using reduction of cytochrome *c* as a monitor, whereas the biosensor method detects a direct physical complex formation without regard to a functional electron transfer. In this context, further investigations have to be performed to elucidate the different steps taking place between the complex formation itself and the electron transfer.

The formation of the AdR-Adx complex alters the midpoint oxidation-reduction potential of the iron-sulfur center by more than 100 mV.[88,100–102] Although the potential of the reductase is approximately −295 mV both in the absence and in the presence of Adx, the potential of Adx changes from −270 mV to approximately −360 mV or less in the complex. The reduced, dissociated state of Adx is then thermodynamically favored compared with the associated state. These data led to the proposal that the reduction of Adx provides the driving force for dissociation of the complex, a crucial property of the physiologic mechanism of electron transfer to the cytochromes P450.[102]

Identification of amino acids on AdR and Adx involved in redox partner recognition

Because negatively charged residues on Adx have been described to be of importance for recognition of AdR (see below), positively charged amino acids on AdR have been suggested to play a role for this interaction. The treatment of bovine AdR with the lysine modifying reagent pyridoxal phosphate led to the modification of Lys243 which inhibited the ability of AdR to transfer electrons to cytochrome *c* by means of Adx.[103,104] Modification of Lys243 as well as inhibition could be suppressed when Adx was present during the chemical modification reaction. Lys243 is located within a dense concentration of basic residues, making this region attractive for interactions with acidic residues of the ferredoxin. Brandt and Vickery[99] performed site-directed mutagenesis of human AdR basic residues in this region, which revealed an interesting result. Replacement of the indicated homologous lysine by glutamine (K242Q) had minor effect on ferredoxin binding. The major effect occurred after replacement of the adjacent Arg243 by glutamine (R243Q). The binding affinity of this mutant for ferredoxin was approximately 1,600-fold

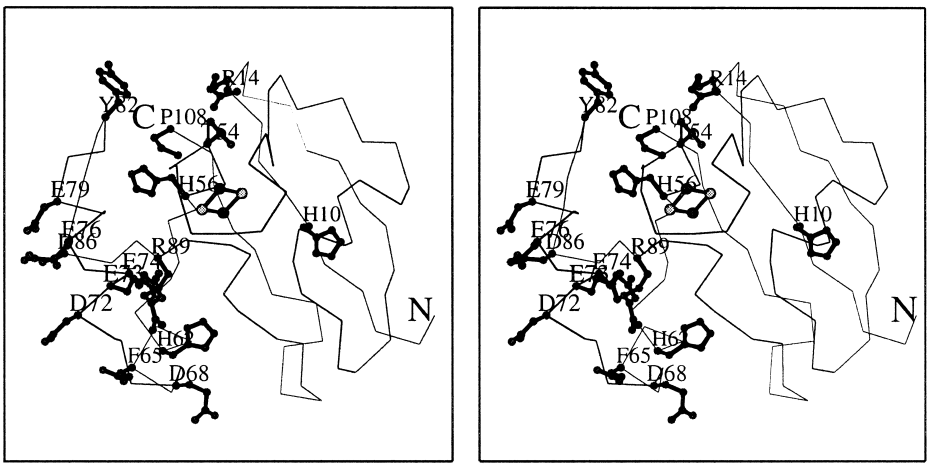

Fig. 7. Stereographic drawing of the Cα trace of Adx(4-108). Residues mutated and discussed in text as well as the [2Fe-2S] cluster are shown in ball-and-stick representation.

reduced. Replacement of Arg239 by serine also had an inhibitory effect, lowering the affinity approximately 17-fold.

Chemical modification of lysine and arginine residues on the surface of Adx had no effect on Adx binding either to AdR or to CYP11A1.[96,105] Similarly, chemical modification of His10 and His62 in adrenodoxin did not influence the interaction with AdR.[127] Additional modification of His56 increased the apparent K_m of Adx for AdR in the cytochrome *c* test two-fold. Modification of free carboxylate groups of aspartate and glutamate residues increased the dissociation constants for binding of AdR and cytochrome CYP11A1 approximately 10 to 20-fold,[105] suggesting that both protein interactions involve the same or overlapping sites on Adx. The role of the unique Tyr82 (Fig. 7) of bovine Adx was examined by a modification with tetranitromethane to give NH_2-Tyr82 and its derivative NO_2-Tyr82. For the modified protein, the cytochrome *c* reduction in the presence of NADPH and AdR were 19% and 9% of the native Adx, respectively. This result implicated that the unique tyrosine residue in Adx is involved either in ET or in the interaction with AdR.[106]

Further investigations of the function of specific residues involved in interaction could be performed by using the technique of site directed mutagenesis. The residues of Adx, which are discussed in this review are depicted in Figure 7. As shown in Table III, the kinetics of bovine wild-type Adx and its mutants T54S, Y82F, Y82S, Y82L, Adx(4-128), Adx(4-107), Adx(4-108A), Adx(4-108S), Adx(4-108W), Adx(4-108K), Adx(4-108)/R14A, Adx(4-108)/R14E, as well as Adx(1-115), which was obtained by trypsin cleavage[107] are quite similar in coupling AdR with cytochrome *c* reduction. They all keep the features of the wild-type Adx in transferring electrons. There are only small changes in the determined kinetic data indicating that C-terminal truncation up to the residue 116 or replacement of amino acids Tyr82 and Thr54 by serine has no significant effect on the interaction with AdR. In contrast, interaction is affected by Adx mutations T54A and Adx(4-114) that show a 65% and a 42% decreased K_m value compared with the wild-type. The V_{max} of the mutants T54A, Adx(4-114) is close to that of wild-type Adx and, together with the decreased K_m values, suggests an increased affinity of these mutants for AdR. Mutants H56Q and H56T display an increase of the K_m of 110%, and 183%, respectively. The K_m of the truncated Adx(4-

TABLE III. Relative Kinetic Constants for the Interactions of Bovine and Human Ferredoxins With Adrenodoxin Reductase†

Fdx variants	K_m^{app}	V_{max}	Reference
Bovine WT-Adx	1.00	1.00	56
Adx(4-128)	0.95	1.04	80
Adx(4-114)	0.58	0.97	80
Adx(1-115)	1.24	1.00	107
Adx(4-108)	1.24	1.66	80
Adx(4-107)	0.85	2.02	64
Adx(4-108A)	1.23	1.51	65
Adx(4-108S)	1.28	1.61	65
Adx(4-108K)	1.28	1.37	65
Adx(4-108W)	1.30	1.31	65
Adx(4-108)/R14A	1.28	2.85	68
Adx(4-108)/R14E	1.83	2.75	68
T54S	0.91	1.13	56
T54A	0.35	0.88	56
Y82F	0.70	1.04	97
Y82S	0.90	1.05	97
Y82L	1.00	1.05	97
H56Q	2.10	1.03	37
H56T	2.80	1.00	37
H56R	5.00	1.00	144
D76E	11.2	1.01	109
Human WT-Fdx	1.00	1.00	81
D68A	1.06	0.99	81
D72A	1.59	0.80	81
D72N	1.44	0.90	81
E73A	1.06	0.96	81
E73Q	1.08	0.93	81
E74Q	1.19	0.75	81
D76N	~116	0.75	81
D76E	~93	n.d.	126
D79A	~110	0.80	81
D79E	5	n.d.	126
D79N	~139	0.93	81

†Data are given relative to WT-Adx and WT-Fdx, respectively. Interactions of adrenodoxin with native electron donor were assayed following the reduction of cytochrome *c* at 550 nm. n.d., not determined.

108) is increased by 23.7% suggesting a decreased affinity of this mutant for the electron donor, but the 66% higher V_{max} discloses a more efficient electron transfer. The mutant D76E shows a dramatic increase in K_m, whereas the respective V_{max} is not affected. Interestingly this decrease in binding of bovine Adx mutant D76E to AdR is, however, more than 10-fold less pronounced compared with that of human Fdx mutant D76E. This finding points to species differences in Adx/AdR interaction and to deficient binding of Adx D76E to AdR in combination with an impaired ability to act as an electron transferring protein.

The mutants of human placenta ferredoxin[67] can be divided into a group of low affinity mutants (D76N, D79A, D79N, and D76E), which demonstrated K_m values that are more than 100-fold higher than for the wild-type in the system with AdR, and a group, including mutants D68A, D72A, D72N, E73A, E73Q, E74Q, and D86A, that display K_m values comparable to that of the wild-type (Table III), whereas D79E reveals a five-fold increased K_m value. The determined V_{max} values for all the mutants of human ferredoxin exhibit no significant changes in the efficiency of cytochrome *c* reduction compared with the wild-type protein. On the basis of the findings with the position 76 and 79 mutants, replacement of aspartate by glutamate at these positions was performed to obtain the mutants D76E and D79E. Even if the negative charge is maintained, the replacement is followed by a remarkable decrease in the binding affinity for the redox partners. D76E and D79E exhibit 93-fold and 5-fold higher K_m values compared with that of the human wild-type ferredoxin. All described mutations in human ferredoxin are located in a highly conserved acidic region. The kinetic data suggest that the two aspartic acid residues in position 76 and 79 are very important for the AdR binding because of the remarkable decreases in the affinity (Table III) after replacement by glutamic acid. Based on these results it has been suggested that the active ET complex in these systems requires specific pairwise electrostatic interactions of fixed geometry to perform recognition and binding of the respective reaction partner (Fig. 6).

Because the reduction of Adx by AdR is significantly faster than the ET from Adx to CYP11A1 and thus not rate limiting, the substrate conversion activity of cytochrome P450 should not be affected by changed affinities of Adx mutants to AdR. Nevertheless, comparing the substrate conversion (Tables Va and Vb) in the CYP11A1-dependent reaction, the human ferredoxin mutants D76 and D79 display dramatically decreased specific activities.

Complex Formation Between Adx and CYP11A1

General remarks

Adrenodoxin binds to CYP11A1 with a distance of 58 Å between cysteine residue 95 of Adx and the heme group of CYP11A1 estimated by Förster energy transfer measurements.[96] The interaction of the two proteins perturbs, among other things, the midpoint potential of both redox centers in the Adx-CYP11A1-cholesterol complex.[108] Bound Adx shifts the redox potential of the heme from −284 mV to −314 mV, thus, making the reduction less favorable. The potential of the iron-sulfur center is also shifted in the same direction, from −273 mV to −291 mV. Consequently, the unfavorable effect of complex formation on the heme redox potential is nearly compensated by a parallel potential shift in the iron-sulfur center.

The activity of Adx toward its native terminal electron acceptors, CYP11A1 and CYP11B1, is mostly investigated by HPLC analysis of the products of the respective hydroxylation reaction[109,110] yielding K_m and V_{max} values for the two reactions described (Table V). CYP11A1 converts cholesterol consuming six reduction equivalents for the side-chain cleavage to produce pregnenolone.[111] Kinetic data presented by Seybert et al.[112] show that maximal side-chain cleavage could be achieved at a ratio of less than one AdR per CYP11A1 molecule under saturating Adx-concentrations. Takikawa et al.[113] found the specific activity of CYP11A1 to be 16 nM pregnenolone/min/mol cytochrome P450 with a K_m^{app} of 120 μM for cholesterol and a K_m^{app} of 1.5 μM for Adx. Their studies showed the pH optimum for CYP11A1 to be at 7.2 and a maximum activity at an ionic strength of 0.1 M.

The binding affinity of Adx to CYP11A1 is usually estimated by optical difference spectroscopy analysis.[62] In this assay, the absorbance changes in the Soret region (393–417 nm, i.e., the low-spin to high-spin shift) that occur upon binding of oxidized Adx and cholesterol to CYP11A1 are determined. The binding of substrate and Adx was shown to be cooperative. Lambeth et al.[114] demonstrated that binding of Adx to CYP11A1 increases binding of cholesterol by a factor of approximately 20 and vice versa. Binding of the oxidized wild-type Adx to its natural electron acceptor CYP11A1 is comparable to that of the reduced form.[108] The K_d of the oxidized and substrate free complex between Adx and CYP11A1 is 600 nM[108] whereas the K_d for the Adx-CYP11A1 complex in the substrate-bound form is approximately 30 nM,[88] being similar to the dissociation constant of the Adx-AdR complex extrapolated to zero ionic strength. Both complexes of Adx, with the electron donor, AdR, and the acceptor, CYP11A1, are salt sensitive, suggesting the charged interactions to play a major role in the assembly of the complexes. Nevertheless, this effect is more pronounced for the Adx-CYP11A1 complex.[115]

The physical complex formation between Adx and CYP11A1 was analyzed very recently by using optical biosensor measurements.[87] The k_{on} value proved to be in the order of $0.2 \cdot 10^6$ $M^{-1}s^{-1}$, whereas the k_{off} value was estimated to be 0.02 s^{-1}. The equilibrium constant k_{eq} ($10.5 \cdot 10^6$ M^{-1}) given for the Adx-CYP11A1 complex is in the same range as reported in previous measurements.[81,116] It has been also demonstrated that the affinity of Adx to CYP11A1, besides being dependent on substrate, is highly dependent on detergents, phospholipids, and pH.[117,118] However, the important effect of detergents and phospholipids on the interaction with the respective redox partners is complex and not completely understood yet.

Identification of groups on Adx and CYP11A1 involved in redox partner recognition

In this section, the effects of chemical modification and site-directed mutagenesis approaches on the interaction of

human placenta ferredoxin and bovine adrenodoxin with CYP11A1 are summarized and discussed regarding the importance of the involved amino acids for the recognition of the respective redox partner protein. The discussed residues of Adx are shown on Figure 7. Interpretation of chemical modification experiments is often ambiguous, because several different factors can lead to a change in protein function as a result of the introduction of a chemical label at the amino-acid residue. Thus, it is difficult to distinguish between a direct, localized effect on function, and the effect of a global, long-range change in conformation accompanying modification. Site-directed mutagenesis studies allow the analysis of individual amino-acid residues but the interpretation of the resulting effects is also subject to the same restrictions as the interpretation of chemical modification results. The most unambiguous conclusions come from modifications/mutations that do not affect function or that can be evaluated by modifications/mutations of the corresponding binding partner protein.

It has been demonstrated by chemical modification that negatively charged amino acids on Adx are essential for the interaction with the redox partners.[105,119] To investigate the role of individual amino-acid residues in placenta Fdx and Adx (86.7% identity in their amino acid sequences) as well as in CYP11A1 by using the technique of site-directed mutagenesis, expression systems for the investigated proteins in *E. coli* have been established.[30,120–122] In effort to identify positively charged amino acids of CYP11A1 that could be involved in the interaction with acidic residues of Adx, both chemical modification and mutagenesis studies have been carried out on bovine CYP11A1. Modifications of CYP11A1 with succinic anhydride resulted in the loss of its ability to interact with Adx, indicating the involvement of lysine residues of the heme protein in the interaction with ferredoxin.[90] Structural analysis of peptides labeled with the radioactive reagent showed 11 of 33 lysine residues of CYP11A1 to be among these residues. Modification with fluorescein isothiocyanate (FITC) and pyridoxal phosphate (PLP) implicated Lys339[123] and Lys343[124] as the key residues involved in binding of Adx. FITC and PLP labeled CYP11A1 showed 85% and 60–98% reduced binding to Adx, respectively. The importance of Lys339 and Lys343 has been further confirmed by site-directed mutagenesis studies. The binding affinities for Adx of substitution mutants containing neutral or acidic residues at these positions were decreased 150- to 600-fold depending on the mutation.[125] K_d variations in this range are in good agreement with investigations of Coghlan and Vickery[81] and Brandt and Vickery, who demonstrated the importance of positively charged residues in human AdR (i.e., Arg239 and Arg243) for the interactions between the redox partners (see the Complex Formation Between Adrenodoxin and Adrenodoxin Reductase section) supporting previous findings for the electrostatic nature of the complex formation. The mutated basic residues Lys339 and Lys343 in CYP11A1 are both conserved as Lys or Arg among mitochondrial P450 enzymes (CYP11B1, CYP11B2, CYP27), which is consistent with their role during molecular recognition of ferredoxins. Modification of lysine residues of Adx to form either negatively charged maleyllysines or positively charged dimethylated lysines had no effect on Adx binding either to AdR or to CYP11A1. Similarly, modification of arginines with p-hydroxyphenyl-glyoxal had no effect on binding interactions, indicating that neither lysine nor arginine residues on the surface of Adx participate in the interaction with both redox partner proteins.[96,105]

By incubating Adx with the water-soluble reagent 1-ethyl-3-[3-dimethyl-aminopropyl] carbodiimide (EDC), free carboxylate groups of aspartate and glutamate residues were modified to bulky, positively charged EDC-methylated groups.[119] Peptide mapping studies indicated that the major residues modified, Glu74, Asp79, and Asp86, are closely clustered on the surface of Adx in the highly conserved acidic region, including residues from position Asp68 to Asp86 (Fig. 2). This modification increased the dissociation constants for binding of AdR and cytochrome CYP11A1 approximately 10- to 20-fold,[105] suggesting that both protein interactions involve the same or overlapping sites on Adx.

With the intent to identify individual residues that are involved in binding, each acidic residue of human placenta

TABLE IV. Relative Binding Affinity of Adrenodoxin for CYP11A1[†]

Fdx variants	K_d	Reference
Bovine WT-Adx	1.00	56
Adx(4-128)	1.12	80
Adx(1-115)	0.66	107
Adx(4-114)	0.52	80
Adx(4-108)	0.32	80
Adx(4-108A)	0.79	65
Adx(4-108S)	0.47	65
Adx(4-108K)	1.07	65
Adx(4-108W)	2.03	65
T54S	0.28	56
T54A	0.76	56
Y82F	0.80	97
Y82S	2.70	97
Y82L	1.60	97
H56Q	1.01	37
H56T	2.60	37
H56R	4.80	109
D76E	10.2	109
Human WT-Fdx	1.00	81
D68A	0.87	81
D72A	3.25	81
D72N	3.12	81
E73A	3.62	81
E73Q	3.87	81
E74Q	0.75	81
D76N	6.25	81
D79A	8.25	81
D79E	1.37	126
D79N	1.37	81
D86A	1.12	81
D76E	7.5	126

[†]The affinities of adrenodoxin mutants were analyzed by optical difference spectroscopy where binding of cholesterol to CYP11A1, facilitated by the binding of adrenodoxin, causes absorbance changes in the Soret region (393-417 nm) of CYP11A1.

Fdx between Asp68 to Asp86 was replaced with the corresponding neutral amide form and/or an alanine residue by site-directed mutagenesis.[81] The influence of amino acid replacements on the binding affinity of Fdx for CYP11A1 was estimated by using optical differential spectroscopy and is summarized in Table IV. The most pronounced changes in the affinity for CYP11A1 could be shown for the human Fdx mutants D76N and D79A with six- to eight-fold higher K_d values compared with the wild-type. Significantly increased K_d values only for CYP11A1 were observed when residues Asp72 and Glu73 were replaced by the corresponding amide or alanine, indicating that the binding sites for both partner proteins, AdR and CYP11A1, overlap and that the binding site for CYP11A1 includes greater relative contributions by additional residues (Fig. 6). Substitution of glutamates at the positions 76 and 79 by aspartates shows also an inhibitory effect on interactions with electron transfer partners.[67] Mutant D76E has a 7.5-fold decreased affinity compared with the wild-type suggesting that the aspartate carboxylate residue at this position is essential and that even minimal changes in geometry reduce its ability to form a stable complex between human placenta ferredoxin and the terminal electron acceptor bovine CYP11A1. The mutant D79E exhibits only minor changes in CYP11A1 binding affinity.

Taken together, these results suggest that Asp76 and Asp79 of human placenta Fdx function as key residues on the surface of the protein for ionic interactions with basic residues on the surface of AdR and CYP11A1. Interestingly, mutant D76E of bovine Adx showed a 10-fold decreased affinity for bovine CYP11A1 and a 11-fold decreased affinity for bovine AdR[97] (Table III). Hence, we can anticipate that also Adx has overlapping sites for the recognition of electron donor and electron acceptor proteins. The decrease in binding to bovine CYP11A1 is in the same range as for the human Fdx mutant D76E.

Determination of a probably changed role of the different Adx mutants in their electron transferring function was investigated by HPLC analysis of the hydroxylation products in the CYP11A1 dependent reaction. The mutants were characterized by Michaelis-Menten kinetics expressed in terms of K_m and V_{max}. Coghlan and Vickery[81,126] divided their mutants of human placenta ferredoxin into three groups depending on the behavior in the CYP11A1 catalyzed reaction (Table V). Mutants D68A and D86A display similar activity compared with the wild-type. Mutants D72A, D72N, E73A, and E73Q show reduced activities in the range of 50% compared with the wild-type, suggesting an important role of these residues for the complex formation of the ferredoxin with one or probably both reaction partners, AdR and CYP11A1. The activity of mutants D76N, D79A, and D79N was very poor and could not be exactly determined. By using higher ferredoxin concentrations for this assay, all mutants were clearly shown to be functionally active, but, nevertheless, their specific activity remained low. This decrease in activity is explained by a decrease in binding affinity to AdR and CYP11A1, which is in good agreement with the kinetic data in the cytochrome *c* assay (Table III) and the spectral binding assay with CYP11A1 (Table IV). Mutant E74Q of human Fdx could not be characterized due to instability under the assay conditions. As described in the Conformational Stability and Folding section, residue Glu74 of bovine Adx plays an essential role in stabilizing the interaction between the cluster-containing core domain and the interaction domain. Mutant D76E of bovine Adx[109] is functionally active but exhibits a higher K_m value compared with the wild-type protein. Summarily, a key role for complex formation has been revealed for

TABLE Va. Relative Steady-State Parameters for Steroid Hydroxylation Reactions Mediated by Bovine Adrenal Ferredoxin†

	CYP11A1		CYP11B1		
Adx variant	K_m	V_{max}	K_m	V_{max}	Reference
WT-Adx	1.00	1.00	1.00	1.00	56
Adx(4-128)	0.96	0.93	1.08	1.01	80
Adx(1-115)	0.26	0.93	0.28	0.83	107
Adx(4-114)	0.21	0.96	0.33	2.14	80
Adx(4-108)	0.32	0.96	0.16	3.58	80
Adx(4-107)	0.25	0.98	n.d.	n.d.	64
Adx(4-108A)	0.80	0.93	n.d.	n.d.	65
Adx(4-108S)	1.22	1.00	n.d.	n.d.	65
Adx(4-108K)	3.32	0.79	n.d.	n.d.	65
Adx(4-108W)	3.41	0.65	n.d.	n.d.	65
Adx(4-108)/R14A	0.48	1.02	n.d.	n.d.	68
Adx(4-108)/R14E	0.50	0.98	n.d.	n.d.	68
T54S	0.20	1.01	0.32	2.36	56
T54A	0.36	0.97	0.53	2.18	56
Y82F	0.70	0.98	0.20	1.09	97
Y82L	1.20	0.96	0.40	0.99	97
Y82S	1.40	0.94	2.70	1.05	97
H56Q	1.20	0.99	6.10	1.02	37
H56T	1.20	1.01	4.10	1.01	37
H56R	3.60	1.01	6.30	1.00	144
D76E	2.60	1.02	3.80	1.00	144

†Catalytic properties of adrenodoxin in CYP11A1- and CYP11B1-dependent substrate conversion were studied by analyzing the products of the respective hydroxylation reactions pregnenolone and corticosterone by HPLC. Data are given relative WT-Adx. n.d., not determined.

TABLE Vb. V_{max} Values for CYP11A1-Dependent Reaction of the Human Placental Ferredoxin and Mutant Proteins [81, 126]

Fdx variant	V_{max}
WT-Fdx	1.00
D68A	0.88
D72A	0.42
D72N	0.40
E73A	0.50
E73Q	0.42
E74Q	Not determined because of instability
D76N	<0.03
D79A	<0.03
D79N	<0.03
D86A	0.76

negatively charged residues in human Fdx, (D72, E73, D76, D79) positively charged lysine residues of CYP11A1 (Lys339 and Lys343 in the mature protein)[125] and AdR (Arg239 and Arg243) and for negatively charged residues in Adx (Fig. 6).

Modification of the histidine residues in adrenodoxin, His10, His56, and His62, with diethylpyrocarbonate (DEP) resulted in a differential effect on binding. Miura et al.[127] described that DEP modification of His10 and His62 did not affect the affinity for redox partners, but further modification of the third residue, His56, resulted in a five-fold increase of the K_d for CYP11A1 similarly to the situation as observed with AdR (see the Identification of Amino Acids on AdR and Adx Involved in Redox Partner Recognition section). These results led to the conclusion that chemical modification of His56 is responsible for the reduction of binding affinities of Adx for redox partners. Attempting to better understand the role of His56 of bovine adrenodoxin in redox partner interactions, and to check the proposal of indispensability of this residue for the electron transfer, the mutant proteins H56T, H56Q, and H56R were designed.[37] The affinity of these mutants for the reductase was decreased (Table III), whereas the dissociation constant of mutant H56T and H56R for CYP11A1 was increased 2.6- and 4.8-fold, respectively. The position 56 mutants of bovine Adx display K_m values comparable to the wild-type protein for H56Q and H56T, whereas H56R has a 3.6-fold higher relative K_m value in the CYP11A1-dependent substrate conversion. The relatively small changes of the binding affinity and activities compared with that of the above mentioned mutants D76E and D79A led to the suggestion that the His-56 residue is only indirectly involved in the binding of redox partners. This conclusion is supported by the crystal structure data of bovine Adx,[40] which indicates that His56 connects the core domain with the interaction domain containing the acidic residues between Asp68 to Asp86 and plays a crucial role in positioning this interaction domain for binding to the reductase and CYP11A1 (Fig. 3).

Because Adx contains no tryptophane residue and only a single tyrosine in its primary sequence, it was tempting to investigate the function of this residue. For this, site directed mutagenesis at Tyr-82 has been performed and amino acid changes Y82F, Y82S, and Y82L were generated.[97] The replacement of Tyr82 did not affect AdR binding, but slightly changed the binding constant to CYP11A1 (up to 2.7-fold) indicating a small influence on cytochrome P450 binding. The replacement revealed no significant changes in the electron transfer capacity of Adx to CYP11A1. In the 3-dimensional structure of Adx, Tyr82 is located close to the putative binding site of redox partners.[40] Hence, mutants of Tyr82 can either directly affect binding of cytochromes P450 or can indirectly induce slight motions of the interacting domain.

The function of the strongly conserved amino acid Thr54 of the bovine Adx was investigated by analyzing the replacement mutants T54A and T54S.[56] Both mutants display a more or less pronounced decrease of the K_d value being lowered 1.3-fold and 3.6-fold, respectively. CYP11A1-dependent substrate conversion assays with the mutants T54S and T54A of bovine Adx has revealed a difference in their behavior from the wild-type showing lowered K_m values (79.5% and 63.5%, respectively) and unchanged V_{max}. This finding might reflect slight rearrangements at the recognition sites caused by the distortion of the H-bond between the hydroxyl group of T54 to the sulfur atom of C52.

The C-terminal part of Adx is proposed to participate in the modulation of the electron transfer properties of the molecule.[80,107] Trypsin-cleaved Adx(1-115) exhibits similar affinity to AdR as wild-type Adx, whereas the affinity to CYP11A1 is increased 1.5-fold.[107] Genetically generated deletion of residues 115-128 or 109-128 influenced greatly the interactions with the electron acceptor CYP11A1, being decreased by the factor 1.9 and 3.1, respectively (Table IV). Mutations of the truncated bovine Adx in position 108 resulted in a minor change in binding behavior toward CYP11A1 for mutant Adx(4-108K) whereas a 1.2-fold or 2.1-fold decrease of the K_d value for the mutants Adx(4-108A) and Adx(4-108S) could be detected. In contrast, the mutation Adx(4-108W) led to a 0.5-fold increase of the binding constant. Truncation of Adx resulted in a 5-fold decreased K_m value for mutant Adx(4-114), a 4-fold decrease for Adx(4-107), and a 3.2-fold decreased K_m for Adx(4-108) in the CYP11A1 dependent reaction. Adx(1-115), which was obtained by limited proteolysis also displays enhanced activity as indicated by the 3.8-fold decreased K_m value for the conversion of cholesterol by CYP11A1. Data obtained for the behavior of Adx(4-128) as well as for Adx(4-108)/R14A and Adx(4-108)/R14E toward CYP11A1 are almost the same as the wild-type data. For all the N- and C-terminally deleted mutants mentioned above the V_{max}(i.e., the efficiency of cholesterol conversion) remains unchanged. Increased Michaelis constants are determined for the mutant proteins Adx(4-108A), Adx(4-108S), Adx(4-108W), Adx(4-108K), and D76E. Especially Adx(4-108W) and Adx(4-108K) show a 3.4-fold and 3.3-fold increased K_m, whereas their V_{max} is lowered by the factor 1.5 and 1.2, respectively, suggesting a decrease in activity (Table V).

For the few mutants, for which K_m values (for conversion of cholesterol to pregnenolone) and K_d values (for Adx binding to CYP11A1) are available, a comparison between both types of data can be performed. Only approximately 50% of the bovine Adx mutants (Adx(4-128), Adx(4-108), Adx(4-108A), Adx(4-108W), Adx(4-108K), T54S, Y82F, Y82L, and H56Q) show a significant correlation between K_m and K_d, whereas the other 50% of the mutants (Adx(4-114), Adx(1-115) Adx(4-108S), T54A, Y82S, H56T, H56R, D76E) display no obvious correlation. Thus, a direct dependency between substrate conversion and Adx binding is not observed.

Complex Formation Between Adx and CYP11B1

The interaction of Adx or the homologous human placenta ferredoxin with bovine CYP11B1 is much less studied than the interaction with CYP11A1. Especially binding constants for the complex formation analogous to the data

TABLE VI. Relative Pre–Steady-State Rate Constants for the Transfer of the First Electron From Adrenodoxin to CYP11A1 and CYP11B1[†]

Adx variant	CYP11A1 (k_{app})	CYP11B1 (k_{app})	Reference
WT-Adx	1.00	1.00	56
Adx(4-128)	1.12	1.25	80
Adx(4-114)	1.20	2.97	80
Adx(4-108)	1.45	4.51	80
T54S	0.87	1.66	56
T54A	0.69	1.68	56
Y82L	0.95	1.10	144
Y82S	0.60	0.71	144
Y82F	1.06	1.20	144
H56R	0.82	0.77	144
H56Q	1.99	0.86	144
H56T	2.11	0.91	144
D76E	0.66	0.96	144

[†]The transfer of the first electron from adrenodoxin to the heme iron of cytochrome P450 was recorded at a single-channel stopped-flow spectrometer by measuring the increase in 450 nm of the ferrous carbon monoxide complex of CYP11A1 and CYP11B1, respectively. Data are given relative to WT-Adx.

available for the AdR:Adx and the Adx:CYP11A1 interaction are not published until now. Bovine CYP11B1 catalyzes the 11β-hydroxylation of 11-deoxycorticosterone to form corticosterone, or of 11-deoxycortisol to produce cortisol. In addition, this enzyme can catalyze the successive 18-hydroxylation and 18-oxidation of corticosterone to produce aldosterone. In human, rat, and mouse adrenals, two enzymes of the CYP11B family, CYP11B1 and CYP11B2, are responsible for the formation of cortisol and aldosterone, respectively.[20] There are no in vitro data available on the interaction of these two enzymes with the respective Adx. By using bovine CYP11B1, mutant T54S shows a 67.8% decrease in K_m, and the conversion rate of 11-deoxycorticosterone to corticosterone is accelerated by 136% as compared with the wild-type Adx, whereas T54A exhibits a 47% decreased K_m and a 118% higher V_{max} value. This finding may point to an enhanced rate of the second ET to CYP11B1.[56] Data in Table VI demonstrate a slightly faster transfer of the first electron to CYP11B1. The Adx(4-114) and Adx(4-108) mutants show also decreased K_m values toward CYP11B1. In contrast to the CYP11A1 reaction, the V_{max} in the CYP11B1 reaction is also affected, which is expressed in a 2-fold higher substrate conversion rate for Adx(4-114) and an even 3.6-fold higher V_{max} for Adx(4-108). Adx(4-128) again was similar to wild-type Adx pointing out a negligible role of the first three amino acids for the presteady-state (Table VI) and steady-state (Table III) characteristics of Adx. The K_m values for the mutant proteins Y82F and Y82L are only 23.5% and 41% compared with the wild-type, whereas the K_m of the Y82S mutant is 170% higher than that of the wild-type. The V_{max} values of the three position-82 mutants remain more or less unaffected, indicating that the replacement of the aromatic by an aliphatic residue does not influence the rate-limiting step. The mutants of His56 display a much more dramatic increase in their relative K_m with an increase up to 510% for H56Q. Nevertheless, the determined V_{max} could not be discriminated from the wild-type, so the maximal substrate conversion is not affected.

With respect to the C-terminal region of Adx, Cupp and Vickery[107] showed that amino acids 116-128 are not essential for the function of Adx, but coupling of Adx(1-115) is more effective compared with the wild-type Adx, which displays a 3.5-fold lower K_m for the CYP11B1 reaction with unchanged V_{max}. This indicates that removal of the C-terminal 13 amino acids enhances the rate of this reaction. In addition, Uhlmann et al.[80] showed that residues 109-115 could be also deleted without impairing the functionality of the protein. Surprisingly, the V_{max} values for corticosterone[80] and aldosterone[128] formation increase when using this mutant indicating an enhanced efficiency of substrate conversion by a factor of 4–5. Taken together, the K_d value for CYP11A1 binding as well as the K_m values for the CYP11A1 and CYP11B1 reactions are decreased for the truncated Adx mutants Adx(4-114) and Adx(4-108) (Tables V and IV). Therefore, it is concluded that the C-terminus of Adx has a greater importance for the interactions with the electron acceptor (CYP11A1/CYP11B1) than for those with the electron donor (AdR).

Data for Adx mutants Y82F, Y82S, and Y82L indicate a correlation of the hydrophobicity of the correspondingly exchanged residue with the affinity of these mutants to CYP11B1. This can be due to a direct interaction with the redox partner or to an indirect motion of the interacting domain of Adx (see the Complex Formation Between Adx and CYP11A1 section). The latter is also the explanation for the weak binding of the His56 mutants. The observed differences between the mutants of Thr54 and the wild-type in their kinetic behavior toward CYP11B1 seem to reflect the fact that the Thr54 substitution results in a slight rearrangement at the Adx surface, which allows to detect a difference in interaction with CYP11A1 and CYP11B1, respectively. These data provide evidence that the molecular recognition between Adx and AdR, CYP11A1, and CYP11B1, respectively, is regulated by unique surface features of each reaction partner.

Transfer of the First Electron to the Cytochrome P450; Comparison of Wild-Type Adx and Mutants

The one-electron transfer from reduced Adx to the Fe(III) of CYP11A1 stabilizes the cytochrome-Adx complex, and the re-oxidized Adx dissociates and returns to the now more favorable and more stable complex with reduced AdR to repeat the redox cycle. Nevertheless, the reduction states of both proteins (Adx as well as CYP11A1) seem to be important for the regulation of ET. Lambeth and Kriengsiri[115] compared the midpoint potentials of different CYP11A1 steroid complexes with their reduction rates and found a good linear correlation between the two observed parameters, suggesting an inherent role of the bound substrate for both the reduction rate of the heme and its oxidation-reduction potential. This finding is in agreement with the theory to describe ET processes.[129]

The transfer of the first electron to cytochromes P450 by the one-electron carrier ferredoxin can be spectroscopically followed, because, upon reduction of the heme Fe(III) to Fe(II) of the respective P450 species, those enzymes bind CO to form a P450-CO complex. The typical absorbance of this complex at 450 nm (in contrast to 420 nm in most other heme proteins) is due to the axial cysteinyl ligand to the heme, which is supplied by the polypeptide chain. Rapid mixing techniques like the stopped-flow method allow to observe an increase in the absorption of the CO complex at 450 nm that occurs during transfer of the first electron to CYP11A1/CYP11B1 by Adx and its mutants.[80,109] The heme iron is locked in this very tight complex with CO; therefore, dissociation is negligible. This complex formation makes the reoxidation of the iron; thus, the transfer of a second electron to it impossible. Lambeth and Pember[108] found that the CO-reduction process is biphasic by using dithionite-reduced Adx. This reaction was not dependent on the Adx concentration. In contrast, Beckert and Bernhardt[109] detected a clear concentration dependence. On the other hand, the putidaredoxin-dependent reduction of CYP101 is known to be monophasic,[130] and in agreement with these results, Uhlmann et al.[80] demonstrated the same phenomenon for the formation of the reduced CYP11A1 and CYP11B1-CO complexes. The reasons for these differences are not clear yet but might be explained by application of different reaction conditions and a different behavior of different sets of mutants as well as by different characteristics of mammalian and bacterial electron transfer systems. It should be also taken into account that the progress in detection and data processing methods during the past 5–10 years might also contribute to a more sensitive evaluation of the performed measurements.

Looking at the apparent rate constants of the first electron transfer from Adx and its mutants to cytochrome P450, substantial differences can be detected. Only minor rate differences are observed (Table VI) upon reduction of CYP11A1 by using the truncated Adx mutants that display a maximal increment of 1.5-fold for the Adx(4-108) mutant. Mutants H56Q and H56R reveal relative apparent rate constants that are approximately two-fold higher as compared with the k_{app} observed for the wild-type. In contrast, the reduction rate of CYP11B1 was accelerated 3- and 4.5-fold with Adx mutants Adx(4-114) and Adx(4-108), respectively, and 1.6-fold by using the Thr54 mutants, whereas the other mutants displayed rate constants similar to those of the wild-type protein.

According to investigations of Beckert and Bernhardt,[109] the dominant factor in determining the ET rate for some Adx mutants is the difference in oxidation-reduction potential between donor and acceptor (i.e., Adx and CYP11A1), whereas the rate constants measured with CYP11B1 revealed no obvious dependency on the redox potential of the Adx mutants. However, there are a few mutants of Adx, which did not fit the linear dependency of the electron transfer rate to CYP11A1 on the redox potential, indicating that other factors like steric parameters became more dominant.

A comparison between k_{app} (Table VI) and the velocity of the substrate conversion (Table V) reveals that the transfer of the first electron to P450 is approximately an order of magnitude faster than the catalyzed hydroxylation reaction. The observed correlation between presteady-state apparent rate constant for the CO reduction and the steady-state maximum velocity for the substrate conversion by the respective cytochromes implicates that the rate limitation in the substrate conversion reaction occurs after the transfer of the first electron to cytochrome P450.

According to Sligar and Gunsalus,[61] the slowest step in camphor hydroxylation is the transfer of the second electron from putidaredoxin to CYP101. This finding is supported by the fact that P450 intermediates are detectable up to the formation of the Fe(III) oxy complex, whereas no catalytic P450 form could be observed after the transfer of the second electron because of the instability and extremely short lifetime of the generated peroxy complex.[20] The only exception is the D252N mutant of CYP101 where a new intermediate was detected that is one-electron reduced from oxy-P450 with an intact dioxygen bond.[131] For the mitochondrial cytochromes P450, the rate-limiting step of the reaction cycle has not been unambiguously defined yet.

More stopped flow kinetic studies that use different Adx and cytochrome P450 mutants as well as substrates are necessary to get deeper insight into the factors driving the transfer of the first electron. Furthermore, new experimental approaches have to be developed to get hold of the second electron transfer step in the mitochondrial P450 systems.

COMPARISON OF PROTEIN-PROTEIN INTERACTIONS IN HOMOLOGOUS VERTEBRATE AND BACTERIAL ELECTRON TRANSFER SYSTEMS

Pdx is a bacterial homolog of Adx, revealing 32.7% protein sequence identity. Because the 3-dimensional structures of Pdx[41] and its electron acceptor, CYP101,[132] are known and a wealth of data on the interaction between Pdx and CYP101 are available, this system is an interesting model for understanding ferredoxin-redox partner interaction in hydroxylating-type systems. The first structure-activity correlation for the redox couple Pdx/CYP101 was presented in the studies on the role of the terminal residue of Pdx, Trp106, which is required for high-affinity binding of Pdx to CYP101.[133,134] Replacement of Trp106 confirmed that the affinity depends on the aromatic character of the residue.[134] A possible region for aromatic-aromatic interaction between the Pdx residue Trp106 and CYP101 is postulated to be near the residues Tyr78 and His352 at the proximal surface of the protein.[51]

Besides the involvement of aromatic residues, ionic interactions have been implicated in the interaction between Pdx and CYP101 by studying the effects of ionic strength on the K_m value for CYP101.[130] The distribution of carboxylates over the surface of the negatively charged Pdx is relatively uniform.[51] Geren et al.[135] investigated the role of specific surface carboxylates of Pdx in the

interactions with putidaredoxin reductase (PdR). Modification with a water-soluble carbodiimide resulted in a loss of interaction with PdR. The most heavily modified carboxyl groups were found to be those of residues 58, 65, 67, and 77, located in the same general region of the protein as those on Adx that were identified as the key residues for ionic interactions with AdR and CYP11A1[67] (Fig. 6).

Residues Asp76 and Asp79 in human Adx (aligned with Gly69 and Glu72 in Pdx) are obviously involved in binding to both partner proteins, whereas mutations of Asp72 and Glu73 (aligned with Glu65 and Arg66 in Pdx) both seem to contribute only to cytochrome P450 binding.[81] In contrast, a mutational study of the negatively charged residues Asp58, Glu65, Glu72, and Glu77 on the corresponding α-helical segment in Pdx revealed no significant role for the electron-transfer reaction to CYP101.[136] Moreover, the structure-based model for CYP101-Pdx interactions presented by Pochapsky et al.[51] indicated that none of the acidic residues of Pdx homologous to those implicated in Adx binding to CYP11A1 and AdR are involved in ionic intermolecular interactions. This model proposed three salt bridges as follows: Arg112 (CYP101) and Asp38 (Pdx), Arg109 (CYP101), and Asp34 (Pdx), Arg79 (CYP101), and the terminal carboxylate group of Trp106 (Pdx) (Fig. 6). The results of mutagenesis studies of the Pdx residues Asp38, Asp34, and Trp106 confirmed the involvement of these residues in binding of CYP101,[137] with minor effects of Asp34 replacement. Consequently, different but overlapping binding sites for ET partners have been proposed also for this P450 system. Substitutions of Asp38 and Asp34 only affect binding of CYP101, but not of PdR; mutation of Cys73 was identified as affecting the interaction with PdR, and replacement of Trp106 influenced binding to both redox partners. The molecular dynamics model proposed the binding region for Pdx to reside in a groove on the proximal heme site of the CYP101 molecule, which contains a high proportion of surface-exposed positively charged residues.[51] Experimental evidence for this model has been gathered by site-directed mutagenesis studies[136-138] as well as in a combined theoretical and experimental study.[139] Roitberg with co-workers[139] predicted two possible electron pathways between Pdx and CYP101 by using Poisson-Boltzmann electrostatic, electron pathway, and molecular dynamics calculations. Experimental data suggest a crucial role of the amino acid couple Asp38 (Pdx)- Arg112 (CYP101) and a minor role for the couple Ser44 (Pdx)-Leu356 (CYP101) for the electron transfer. Because the 3-dimensional structure of AdR was published recently,[18] a similar model of the electron transfer complex between Adx and AdR can be derived and respective calculations of the probable electron transfer pathways are under way in our laboratory.

Taken together, for both systems, the bovine mitochondrial steroid hydroxylation system and the bacterial camphor hydroxylation system, specific interactions of redox partners have been identified by site-directed mutagenesis. Pdx and Adx seem to have separate but overlapping binding sites for their respective ET partners. So far no homologous residues on the surface of Adx and Pdx have been found that are involved in the binding process. The differences between the proteins may reflect the distinction in the specificity for reductases and cytochromes of the two ferredoxins, which is also supported by the low cross-reactivity between the reductases[135] and by the incompatibility of the ferredoxins as effector for turnover in the other system.[140]

CONCLUSION

The very recently determined first X-ray structure of a vertebrate-type ferredoxin, the truncated adrenodoxin Adx(4-108),[40] as well as the resolution of the X-ray structure of the full length wild-type Adx,[17] is of great importance not only for better understanding the structure-function relationships and the stabilization of this protein, but also for understanding the biochemistry and biophysics of ferredoxins of the [2Fe-2S] type in general. It could be demonstrated that Adx(4-108) shows a higher similarity in its three-dimensional structure to plant-type ferredoxins than could be deduced from the sequence homology between these proteins whose level of amino-acid identity remains at less than 25%. Essentially, the same fold as for other ferredoxins of the [2Fe-2S] type, the so-called β-grasp motif, has been found. There is significant similarity of the three-dimensional structures in the core region of the proteins with larger deviations in the so-called interaction domains. [19] Because so far only 3-dimensional structures of plant-type ferredoxins and of putidaredoxin, where the immediate surroundings of the [2Fe-2S] cluster had to be modeled, were available, this new structure can serve as a model for deriving the structures of other ferredoxins, especially of the vertebrate-type, by either molecular replacement of X-ray crystallographic data or of data from NMR analysis. In fact, the 3-dimensional structure of putidaredoxin has been refined very recently, and the X-ray structure of full-length Adx has been resolved by molecular replacement by using the coordinates of mutant Adx(4-108).[17,44] Because in the full-length Adx only three additional amino acids compared with Adx(4-108) can be assigned, the wild-type structure cannot explain the reported changes in the interactions of the truncated Adx(4-108) with CYP11A1 and the improved electron transfer to CYP11B1[80] compared with full-length wild-type protein. However, the observed dimerization of Adx showing that the C-terminal part of each of the Adx molecules involved therein extends like an arm over the other molecule coming close to the region containing the residues required for interaction with P450 can explain why truncation affects affinity of Adx for CYP11A1 and CYP11B1.[17] Moreover, the flexible C-terminal tail of human ferredoxin has been demonstrated to undergo a disorder-to-order transition upon reduction of the ferredoxin[141] and, thus, may push the redox partner away as a consequence of the conformational change that accompanies reduction/oxidation of the protein. However, more studies are required to evaluate the full extent of involvement of the C-terminal part in redox partner interaction and electron transfer. Thus, the X-ray structure of reduced Adx would be of great interest to follow structural changes in the cluster environment and in the interplay between the cluster-containing core region and the interaction domain. A refined compari-

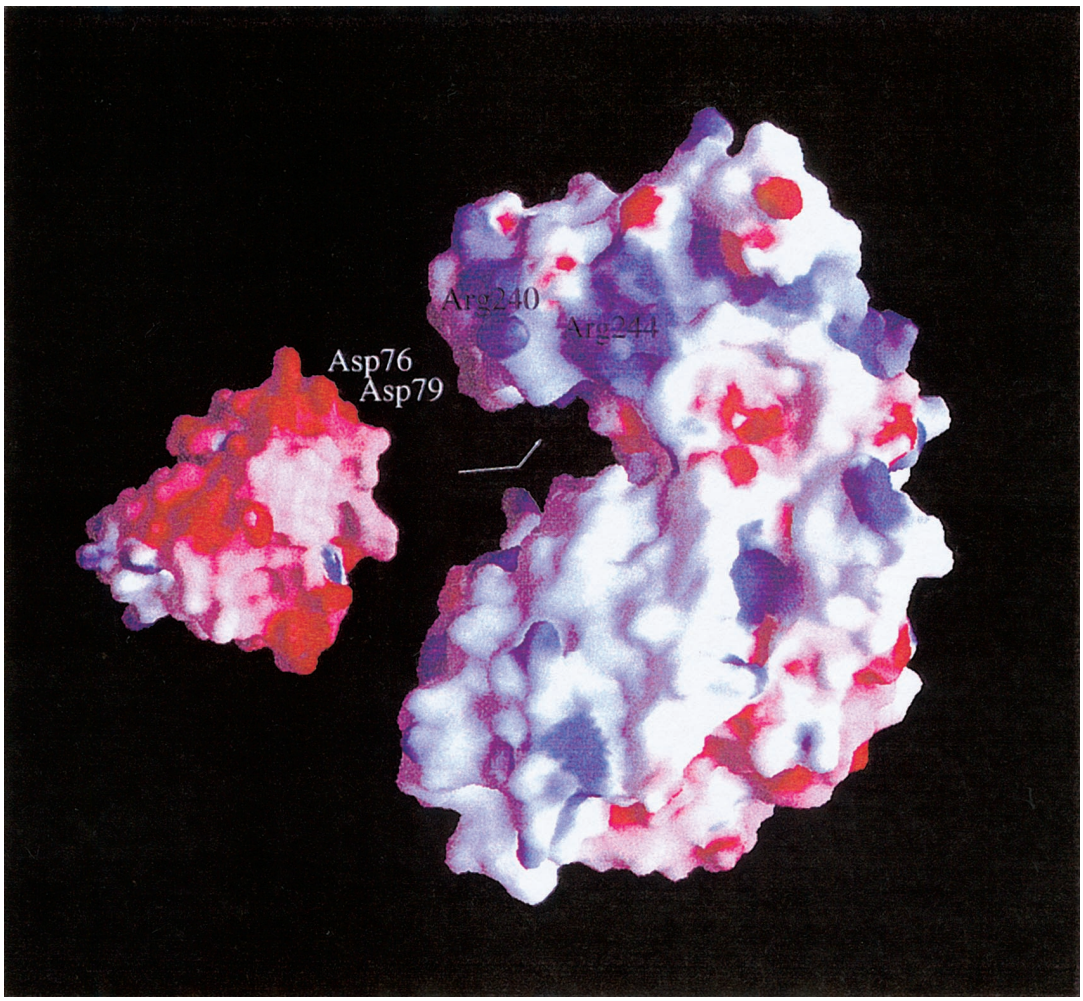

Fig. 8. Surface representation of adrenodoxin and adrenodoxin reductase colored according to the electrostatic potential from blue (positive) to red (negative). Adx fits into a groove of AdR thereby matching the negative and positive potentials. The interacting residues are labeled. The figure was drawn by using GRASP.[147]

son between the structures of oxidized and reduced Adx and Pdx probably could also give an answer on the so far poorly understood observation that Adx, although being 32.7% identical with Pdx in the amino acid sequence, is not able to transfer the second electron to the camphor-hydroxylating CYP101. In this connection, a 3-dimensional structure of an electron transfer complex of proteins from cytochrome P450 systems would clearly help to better understand the principle of electron transfer in these enzyme systems and the pathway(s) the electron moves from one redox center to the other, and would indicate possibilities to regulate this step. Such a structure, together with site-directed mutagenesis studies would help to identify amino-acid residues being involved in the main function of this protein, electron transfer. These data could also provide valuable information on the molecular basis for the various redox potentials in different ferredoxins and their mutants and on the interrelationship between the redox potential and the rate of the two electron-transfer steps. The results so far available on the structure and the importance of individual amino-acid residues for the function of Adx (and Pdx) gives us an idea on the region(s) involved in redox-partner binding. It remains, however, an open question, whether the differences, which have been described for these binding sites between Adx and Pdx rather reflect different binding requirements or whether more than one region is involved in redox-partner interaction in both proteins. Further mutagenesis and binding studies and, of course, the 3-dimensional structures of the different electron-transfer complexes will answer this question.

Because very recently the 3-dimensional structure of AdR became available, a model of Adx/AdR recognition has been derived, taking into account the different surfaces and charges of both proteins as well as data from modification and site-directed mutagenesis studies (Fig. 8). Attempts to crystallize this complex are under way. In addition, site-directed mutagenesis studies of potential interaction sites will lead to deeper insight

into the similarities and differences in the requirements of Adx binding of the various redox partners. A comparison of Adx binding to other mitochondrial cytochromes P450, besides CYP11A1 and CYP11B1, surely will reveal further details in protein-protein recognition and electron transfer in different P450 systems.

Another unresolved problem is the folding pathway of Adx and the understanding of the forces leading to stabilization of the Adx structure. Recently, first results of investigations on the conformational stability and folding of Adx became available.[77,78] The developed method allows to study also other ferredoxins of the [2Fe-2S] type and can help to characterize the thermodynamic behavior of this interesting protein class. The main problem with these studies is that the iron-sulfur cluster is rather unstable and tends to dissociate before unfolding of the polypeptide chain, if no protective conditions are applied. It has to be mentioned that even under the protective conditions used so far the refolding never reaches 100% as observed for the classic model proteins without prosthetic group (lysozyme, β-lactoglobulin, barnase, RNases A and T1) or with a covalently bound prosthetic group (cytochrome *c*). Nevertheless, at up to 85% refolding, reliable thermodynamic data can be derived studying the unfolding/refolding of Adx and its mutants. By using this method, the role of a hydrogen bond between Pro108 and Arg14 and of the salt bridge between Glu74 and Arg89 for Adx stability has been defined. The kinetics of unfolding/refolding, the in vivo folding and the time, compartment and mechanism of the [2Fe-2S] cluster uptake are not understood yet and need further investigation. The data obtained so far do not exclude association of the [2Fe-2S] cluster to partially unfolded Adx, thus, rendering an import of the intact Adx with cluster from the cytoplasm to the mitochondrial matrix in principle possible.

Taken together, the structural, functional, and thermodynamic data obtained within the past 5–10 years on Adx lead to new insights not only to understand this electron transfer protein and the reactions, where it participates, but also to understand other ferredoxins of the [2Fe-2S] type much better. However, there are still many open questions waiting to be resolved. It can be expected that rationally designed experiments that use the knowledge of the 3-dimensional structures of different ferredoxins and, as soon as they will be available, new structural data on ferredoxins and their electron transfer complexes, will lead to deeper insights into the structure and function of this protein class and of the biological systems they are involved in.

ACKNOWLEDGMENT

R.B. and U.H. received grants from the Deutsche Forschungsgemeinschaft and the Fonds der Chemischen Industrie.

REFERENCES

1. Peterson JA, Lu J-Y, Geisselsoder J, Graham-Lorence S, Carmona C, Witney F, Lorence MC. Cytochrome P-450terp Isolation and purification of the protein and cloning and sequencing of its operon. J Biol Chem 1992;267:14193–14203.
2. Hedegaard J, Gunsalus IC. Mixed function oxidation IV An induced methylene hydroxylase in camphor oxidation. J Biol Chem 1965;240:4038–4043.
3. Matsubara H, Saeki K. Structural and functional diversity of ferredoxins and related proteins. Adv Inorg Chem 1992;38:223–280.
4. Rypniewski WR, Breiter DR, Benning MM, Wesenberg G, Oh BH, Markley JL, Rayment I, Holden HM. Crystallization and structure determination to 25-Å resolution of the oxidized [2Fe-2S] ferredoxin isolated from *Anabaena.* 7120 Biochemistry 1991; 30,4126–4131.
5. Jacobson BL, Chae YK, Markley JL, Rayment I, Holden HM. Molecular structure of the oxidized, recombinant, heterocyst [2Fe-2S] ferredoxin from *Anabaena 7120* determined to 17 Å resolution. Biochemistry 1993;32:6788–6793.
6. Tsukihara T, Fukuyama K, Nakamura M, Katsube Y, Tanaka N, Kakudo M, Wada K, Hase T, Matsubara H. X-ray analysis of a [2Fe-2S] ferredoxin from *Spirulina platensis.* Main chain fold and location of side chains at 25 Å resolution. J Biochem 1981;90:1763–1773.
7. Tsukihara T, Fukuyama K, Mitsushima M, Harioka T, Kusunoki M, Katsube Y, Hase T, Matsubara H. Structure of the [2Fe-2S] ferredoxin I form the blue green algae *Aphanothece sacrum* at 22 Å resolution. J Mol Biol 1990;216;399–410.
8. Binda C, Coda A, Aliverti A, Zanetti G, Mattevi A. Structure of the mutant E92K of [2Fe-2S] ferredoxin I from *Spinacia oleracea* at 17 Å resolution. Acta Crystallogr 1998;D54:1353–1358.
9. Ikemizu S, Bando M, Sato T, Morimoto Y, Tsukihara T, Fukuyama K. Structure of [2Fe-2S] ferredoxin I from *Equisetum avense* at 18 Å resolution. Acta Crystallogr 1994;D50:167–174.
10. Hurley JK, Weber-Main AM, Stankovich MT, Benning MM, Thoden JB, Vanhooke JL, Holden HM, Chae YK, Xia B, Cheng H, Markley JL, Martinez Julvez M, Gomez-Moreno C, Schmeits JL, Tollin G. Structure-function relationships in *Anabaena* ferredoxin: correlation between X-ray crystal structures, reduction potentials, the rate constants of electron transfer to ferredoxin: NADPH reductase for site-directed mutants. Biochemistry 1997; 36:11100–11117.
11. Xiao Z, Lavery ML, Ayhan M, Scrofani SDB, Wilce MCJ, Guss JM, Tregloan PA, George GN, Wedd AG. The rubredoxin from *Clostridium pasteurianum*: mutation of the iron cysteinyl ligands to serine Crystal and molecular structure of oxidized and dithionite-treated forms of the Cys42Ser mutant. J Am Chem Soc 1998;120:4135–4150.
12. Gomez-Moreno C, Martinez-Julvez M, Fillat MF, Hurley JK, Tollin G. Molecular recognition in protein complexes involved in electron transfer. Biochem Soc Trans 1996;24:111–116.
13. Hurley JK, Hazzard JT, Martinez-Julvez M, Medina M, Gomez-Moreno C, Tollinn G. Electrostatic forces involved in orienting *Anabaena ferredoxin* during binding to Anabaena ferredoxin NADP+ reductase: site-specific mutagenesis, transient kinetic measurements, and electrostatic surface potentials. Protein Sci 1999;8:1614–1622.
14. Matsubara H, Wada K, Masaki R. Structure and function of chloroplast-type ferredoxins. Adv Exp Med Biol 1976;74:1–15.
15. Hurley JK, Schmeits JL, Genzor C, Gomez-Moreno C, Tollin G. Charge reversal mutations in a conserved acidic patch in *Anabaena* ferredoxin can attenuate or enhance electron transfer to ferredoxin NADP+ reductase by altering protein-protein orientation within the intermediate complex. Arch Biochem Biophys 1996;333:243–250.
16. Holden HM, Jacobson BL, Hurley JK, Tollin G, Oh BH, Skjeldal L, Chae YK, Cheng H, Xia B, Markley JL. Structure-function studies of [2Fe-2S] ferredoxins. J Bioenerg Biomembr 1994;26: 167–188.
17. Pikuleva IA, Tesh K, Waterman MR, Kim Y. The tertiary structure of full-length bovine adrenodoxin suggests functional dimers. Arch Biochem Biophys 2000;373:44–55.
18. Ziegler GA, Vonrhein C, Hanukoglu I, Schulz GE. The structure of adrenodoxin reductase of mitochondrial P 450 Systems: electron transfer for steroid biosynthesis. J Mol Biol 1999;289:981–990.
19. Muller JJ, Muller A, Rottmann M, Bernhardt R, Heinemann U. Vertebrate-type and plant-type ferredoxins: crystal structure comparison and electron transfer pathway modelling. J Mol Biol 1999;294:501–513.
20. Bernhardt R. Cytochrome P450: structure, function, and genera-

tion of reactive oxygen species. Rev Physiol Biochem Pharmacol 1996;127:137–221.
21. Matocha MF, Waterman MR. Discriminatory processing of the precursor forms of cytochrome P-450scc and adrenodoxin by adrenocortical and heart mitochondria. J Biol Chem 1984;259: 8672–8678.
22. Moulis J-M, Davasse V, Golinelli M-P, Meyer J, Quinkal I. The coordination sphere of iron-sulfur clusters: lessons from site-directed mutagenesis experiments. J Biol Inorg Chem 1996;1:2–14.
23. Beinert H, Kennedy MC. Aconitase, a two-faced protein: enzyme and iron-regulatory factor. FASEB J 1993;7:1442–1449.
24. Brereton PS, Duderstadt RE, Staples CR, Johnson MK, Adams MW. Effect of serinate ligation at each of the iron sites of the [Fe4S4] cluster of *Pyrococcus furiosus* ferredoxin on the redox, spectroscopic, and biological properties. Biochemistry 1999;38: 10594–10605.
25. Gurbiel RJ, Batie CJ, Sivaraja M, True AE, Fee JA, Hoffman BM, Ballou DP. Electron-nuclear double resonance spectroscopy of 15N-enriched phthalate dioxygenase from *Pseudomonas cepacia* proves that two histidines are coordinated to the [2Fe-2S] Rieske-type clusters. Biochemistry 1989;28:4861–4871.
26. Werth MT, Cecchini G, Manodori A, Ackrell BA, Schroder I, Gunsalus RP, Johnson MK. Site-directed mutagenesis of conserved cysteine residues in *Escherichia coli* fumarate reductase: modification of the spectroscopic and electrochemical properties of the [2Fe-2S] cluster. Proc Natl Acad Sci USA 1990;87:8965–8969.
27. Xia B, Cheng H, Bandarian V, Reed GH, Markley JL. Human ferredoxin: overproduction in *Escherichia coli*, reconstitution in vitro, and spectroscopic studies of iron-sulfur cluster ligand cysteine-to-serine mutants. Biochemistry 1996;35:9488–9495.
28. Meyer J, Fujinaga J, Gaillard J, Lutz M. Mutated forms of the [2Fe-2S] ferredoxin from *Clostridium pasteurianum* with noncysteinyl ligands to the iron-sulfur cluster. Biochemistry 1994;33: 13642–13650.
29. Hurley JK, Weber-Main AM, Hodges AE, Stankovich MT, Benning MM, Holden, HM, Cheng H, Xia B, Markley JL, Genzor C, Gomez-Moreno C, Hafezi R, Tollin G. Iron-sulfur cluster cysteine-to-serine mutants of *Anabaena* [2Fe-2S] ferredoxin exhibit unexpected redox properties and are competent in electron transfer to ferredoxin:NADP+ reductase. Biochemistry 1997;36:15109–15117.
30. Uhlmann H, Beckert V, Schwarz D, Bernhardt R. Expression of bovine adrenodoxin and site-directed mutagenesis of [2Fe-2S] cluster ligands. Biochem Biophys Res Commun 1992;188:1131–1138.
31. Estabrook RW, Suzuki K, Mason JI, Baron J, Taylor WE, Simpson JP, Purvis J, McCarthy J. Adrenodoxin: an iron-sulfur protein of adrenal cortex mitochondria In: Lovenberg W, editor. Iron-sulfur proteins. Vol. 2. New York: Academic Press; 1973. p 193–223.
32. Meyer J, Moulis JM, Lutz M. Structural differences between [2Fe-2S] clusters in spinach ferredoxin and in the "red paramagnetic protein" from *Clostridium pasteurianum.* A resonance Raman study. Biochem Biophys Res Commun 1984;119:828–835.
33. Han S, Czernuszewicz RS, Kimura T, Adams MWW, Spiro TG. [2Fe-2S] protein resonance Raman spectra revisited: structural variations among adrenodoxin, ferredoxin and red paramagnetic protein. J Am Chem Soc 1989;111:3505–3511.
34. Cammack R, Rao KK, Hall DO, Johnson CE. Mossbauer studies of adrenodoxin. The mechanism of electron transfer in a hydroxylase iron-sulphur protein. Biochem J 1971;125:849–856.
35. Mukai K, Kimura T, Helbert J, Kevanl L. Environment of the iron-sulfur chromophore in adrenodoxin studied by EPR and ENDOR spectroscopy. Biochim Biophys Acta 1973;295:49–56.
36. Miura S, Ichikawa Y. Conformational change of adrenodoxin induced by reduction of iron-sulfur cluster. Proton nuclear resonance study. J Biol Chem 1991;266:6252–6258.
37. Beckert V, Schrauber H, Bernhardt R, Van Dijk AA, Kakoschke C, Wray V. Mutational effects on the spectroscopic properties and biological activities of oxidized bovine adrenodoxin, and their structural implications. Eur J Biochem 1995;231:226–235.
38. Cammack R, Rao KK, Hall DO. Metalloproteins in the evolution of photosynthesis. Biosystems 1981;14:57–80.
39. Bairoch A, Bucher P, Hofmann K. The PROSITE database, its status in 1997. Nucleic Acids Res 1997;25:217–221
40. Müller A, Müller JJ, Muller YA, Uhlmann H, Bernhardt R, Heinemann U. New aspects of electron transfer revealed by the crystal structure of a truncated bovine adrenodoxin, Adx(4-108). Structure 1998;6:269–280.
41. Pochapsky TC, Ye XM, Ratnaswamy G, Lyons TA. An NMR-derived model for the solution structure of oxidized putidaredoxin, a [2Fe-2S] ferredoxin from *Pseudomonas putida.* Biochemistry 1994;33:6424–6432.
42. Mo H, Pochapsky SS, Pochapsky TC. A model for the solution structure of oxidized terpredoxin, a FE2S2 ferredoxin from Pseudomonas. Biochemistry 1999;38:5666–5675.
43. Miura S, Ichikawa Y. Proton nuclear magnetic resonance investigation of adrenodoxin. Assignment of aromatic resonances and evidence for a conformational similarity with ferredoxin from *Spirulina platensis.* Eur J Biochem 1991;197:747–775.
44. Pochapsky TC, Jain NU, Kuti M, Lyons TA, Heymont J. A refined model for the solution structure of oxidized putidaredoxin. Biochemistry 1999;38:4681–4690.
45. Bernstein FC, Koetzle TF, Williams GJ, Meyer EE Jr, Brice MD, Rodgers JR, Kennard O, Shimanouchi T, Tasumi M. The protein data bank: a computer-based archival file for macromolecular structures. J Mol Biol 1977;112:535–542.
46. Sussman JL, Shoham M, Harel M. Protein adaptation to extreme salinity: the crystal structure of 2Fe-2S ferredoxin from *Halobacterium marismortui.* Prog Clin Biol Res 1989;289:171–187.
47. Baumann B, Sticht H, Scharpf M, Sutter M, Haehnel W, Rosch P. Structure of *Synechococcus elongatus* [Fe_2-S2] ferredoxin in solution. Biochemistry 1996;35:12831–12841.
48. Hatanaka H, Tanimura R, Katoh S, Inagaki F. Solution structure of ferredoxin from the thermophilic cyanobacterium *Synechococcus elongatus* and its thermostability. J Mol Biol 1997;268:922–933.
49. Bes MT, Parisini E, Inda LA, Saraiva L, Peleato ML, Sheldrick GM. Crystal structure determination at 14 Å resolution of ferredoxin from the green algae *Chlorella fusca.* Structure 1999; 7:1201–1211.
50. Overington JP. Comparison of the three-dimensional structures of homologous proteins. Curr Opin Struct Biol 1992;2:394–401.
51. Pochapsky TC, Lyons TA, Kazanis S, Arakaki T, Rasnaswamy G. A structure-based model for cytochrome P450cam-putidaredoxin interactions. Biochimie 1996;78:723–733.
52. Dugad LB, La-Mar GN, Banci L, Bertini I. Identification of localized redox states in plant-type two-iron ferredoxins using the nuclear Overhauser effect. Biochemistry 1990;29:2263–2271.
53. Stephens PJ, Jollie DR, Warshel A. Protein control of redox potentials of iron-sulfur proteins. Chem Rev 1996;96:2491–2513.
54. Bertrand P, Gayda JP. A theoretical interpretation of the variations of some physical parameters within the [2Fe-2S] ferredoxin group. Biochim Biophys Acta 1979;579:107–121.
55. Fu W, Drozdzewski PM, Davies MD, Sligar SG, Johnson MK. Resonance Raman and magnetic circular dichroism studies of reduced [2Fe-2S] proteins. J Biol Chem 1992;267:15502–15510.
56. Uhlmann H, Bernhardt R. The role of threonine 54 in adrenodoxin for the properties of its iron-sulfur cluster and its electron transfer function. J Biol Chem 1995;270:29959–29966.
57. Adman E, Waternpaugh KD, Jensen LH. NH–S hydrogen bonds in *Peptococcus aerogenes* ferredoxin, *Clostridium pasteurianum* rubredoxin, and *Chromatium* high potential iron protein Proc Natl Acad Sci USA 1975;72:4854–4858.
58. Langen R, Jensen GM, Jacob U, Stephens PJ, Warshel A. Protein control of iron-sulfur cluster redox potentials. J Biol Chem 1992;267:25625–25627.
59. Bertrand P, Mbarki O, Asso M, Blanchard L, Guerlesquin F, Tegoni M. Control of the redox potential in c-type cytochromes: importance of the entropic contribution. Biochemistry 1995;34: 11071–11079.
60. Kassner RJ. Effects of nonpolar environments on the redox potentials of heme complexes. Proc Natl Acad Sci USA 1972;69: 2263–2267.
61. Sligar SG, Gunsalus IC. Proton coupling in the cytochrome P-450 spin and redox equilibria. Biochemistry 1979;18:2290–2295.
62. Kido T, Kimura T. The formation of binary and ternary complexes of cytochrome P-450scc with adrenodoxin and adrenodoxin reductase-adrenodoxin complex. The implication in ACTH function. J Biol Chem 1979;254;11806–11815.

63. Correll CCX, Batie CJ, Ballou DP, Ludwig ML. Phthalate dioxygenase reductase: a modular structure for electron transfer from pyridine nucleotides to [2Fe-2S]. Science 1992;258:1604–1610.
64. Uhlmann H, Iametti S, Vecchio G, Bonomi F, Bernhardt R. Pro108 is important for folding and stabilization of adrenal ferredoxin, but does not influence the functional properties of the protein. Eur J Biochem 1997;248:897–902.
65. Grinberg A, Bernhardt R. Effect of replacing a conserved proline residue on the function and stability of bovine adrenodoxin. Protein Eng 1998;11:1057–1064.
66. Castro G, Boswell CA, Northrup SH. Dynamics of protein-protein docking: cytochrome c and cytochrome peroxidase revisited. J Biomol Struct Dyn 1998;16:413–424.
67. Vickery LE. Molecular recognition and electron transfer in mitochondrial steroid hydroxylase systems. Steroids 1997;62:124–127.
68. Grinberg A, Bernhardt R. Structural and functional consequences of substitutions at the Pro108-Arg14 hydrogen bond in bovine adrenodoxin. Biochem Biophys Res Commun 1998;249:933–938.
69. Iametti S, Uhlmann H, Ragg E, Sala N, Grinberg A, Beckert V, Bernhardt R, Bonomi F. Cluster-iron substitutions is related to structural and functional features of adrenodoxin mutants and to their redox states. Eur J Biochem 1998;251:673–681.
70. Uhlmann H. Die Rolle von Threonin-54, Cystein-Resten sowie der N- und C-terminalen Bereiche des adrenalen Ferredoxins für seine Funktion als Elektronenüberträger. PhD Thesis, Humboldt Universität, Berlin; 1995.
71. Grinberg A. Untersuchungen zur Stabilitaet und zum Faltungsmechanismus des bovinen adrenalen Ferredoxins. PhD Thesis, Universitaet des Saarlandes, Saarbruecken; 1998.
72. Padmanabhan R, Kimura T. Extrinsic properties of optical activity in adrenal iron-sulfur protein (adrenodoxin). Biochem Biophys Res Commun 1969;37:363–366.
73. Petering D, Fee JA, Palmer G. The oxygen sensitivity of spinach ferredoxin and other iron-sulfur proteins. The formation of protein-bound sulfur-zero. J Biol Chem 1971;246:643–653.
74. Padmanabhan R, Kimura T. Studies on adrenal steroid hydroxylases. Extrinsic properties of the optical activity in adrenal iron-sulfur protein (adrenodoxin). J Biol Chem 1970;245:2469–2475.
75. Pagani S, Bonomi F, Cerletti P. Enzymatic synthesis of the iron-sulfur cluster of spinach ferredoxin. Eur J Biochem 1984;142:361–366.
76. Bera AK, Grinberg A, Bernhardt R. A step toward understanding the folding mechanism of bovine adrenodoxin: reversible unfolding/refolding under aerobic conditions. Arch Biochem Biophys 1999;361:315–322.
77. Burova TV, Bernhardt R, Pfeil W. Conformational stability of bovine holo and apo adrenodoxin: a scanning calorimetric study. Protein Sci 1995;4:909–916.
78. Burova TV, Beckert V, Uhlmann H, Ristau O, Bernhardt R, Pfeil W. Conformational stability of adrenodoxin mutant proteins. Protein Sci 1996;5:1890–1897.
79. Privalov PL. Stability of proteins: small globular proteins. Adv Protein Chem 1979;33:167–240.
80. Uhlmann H, Kraft R, Bernhardt R. C-terminal region of adrenodoxin affects its structural integrity and determines differences in its electron transfer function to cytochrome P-450. J Biol Chem 1994;269:22557–22564.
81. Coghlan VM, Vickery LE. Site-specific mutations in human ferredoxin that affect binding to ferredoxin reductase and cytochrome P450scc. J Biol Chem 1991;266:18606–18612.
82. Perutz MF, Raidt H. Stereochemical basis of heat stability in bacterial ferredoxins and in haemoglobin A2. Nature 1975;255:256–259.
83. Goder V, Beckert V, Pfeil W, Bernhardt R. Impact of the presequence of amitochondrium-targeted precursor, preadrenodoxin, on folding, catalytic activity and stability of the protein in vitro. Arch Biochem Biophys 1998;359:31–41.
84. Bera AK, Bernhardt R. GroEL-assisted and -unassisted refolding of mature and precursor adrenodoxin: the role of the precursor sequence. Arch Biochem Biophys 1999;367:89–94.
85. Kimura T. ACTH stimulation on cholesterol side chain cleavage activity of adrenocortical mitochondria. Transfer of the stimulus from plasma membrane to mitochondria. Mol Cell Biochem 1981;36:105–122.
86. Akhrem AA, Lapko VN, Lapko AG, Shkumatov VM, Chashchin VL. Isolation, structural organization and mechanism of action of mitochondrial steroid hydroxylating systems. Acta Biol Med Ger 1979;38:257–273.
87. Ivanov YD, Usanov SA, Archakov AI. Optical biosensor studies on the productive complex formation between the components of cytochrome P450scc dependent monooxygenase system. Biochem Mol Biol Int 1999;47:327–336.
88. Lambeth JD, Seybert DW, Lancaster JR Jr, Salerno JC, Kamin H. Steroidogenic electron transport in adrenal cortex mitochondria. Mol Cell Biochem 1982;45:13–31.
89. Schwarz D, Chernogolov A, Kisselev P. Complex formation in vesicle-reconstituted mitochondrial cytochrome P450 systems (CYP11A1 and CYP11B1) as evidenced by rotational diffusion experiments using EPR and ST-EPR. Biochemistry 1999;38:9456–9464.
90. Adamovich TB, Pikuleva IA, Chashchin VL, Usanov SA. Selective chemical modification of cytochrome P-450SCC lysine residues. Identification of lysines involved in the interaction with adrenodoxin. Biochim Biophys Acta 1989;996:247–253.
91. Takeshima M, Hara T. High density lipoprotein cholesterol as a mechanistic probe for the side chain cleavage reaction. Biochem Biophys Res Commun 1991;179:161–169.
92. Hara T, Takeshima M. Conclusive evidence of a quartery cluster model for cholesterol side chain cleavage reaction catalyzed by cytochrome P450scc. In: Lechner MC, editor. Cytochrome P450 8th International Conference. Paris: John Libbey Eurotext; 1994. p 417–420.
93. Chu J-W, Kimura T. Studies on adrenal steroid hydroxylases: molecular and catalytic properties of adrenodoxin reductase (a flavoprotein). J Biol Chem 1973;248:2089–2094.
94. Lambeth JD, Kamin H. Adrenodoxin reductase. Properties of the complexes of reduced enzyme with NADP+ and NADPH. J Biol Chem 1976;251:4299–4306.
95. Lambeth JD. Enzymology of mitochondrial side-chain cleavage by CYP450scc. In: Ruckpaul K, Rein H, editors. Fronts biotransformations. Berlin: Akademie-Verlag; 1990. p 58–99.
96. Tuls J, Geren L, Lambeth JD, Millett F. The use of a specific fluorescence probe to study the interaction of adrenodoxin with adrenodoxin reductase and cytochrome P-450scc. J Biol Chem 1987;262:10020–10025.
97. Beckert V, Dettmer R, Bernhardt R. Mutations of tyrosine 82 in bovine adrenodoxin that affect binding to cytochromes P45011A1 and P-45011B1 but not electron transfer. J Biol Chem 1994;269:2568–2573.
98. Lambeth JD, Kamin H. Adrenodoxin reductase: adrenodoxin complex Flavin to iron-sulfur transfer as the rate-limiting step in NADPH-cytochrome c reductase reaction. J Biol Chem 1979;254:2766–2774.
99. Brandt ME, Vickery LE. Charge pair interactions stabilizing ferredoxin-ferredoxin reductase complexes. Identification by complementary site-specific mutations. J Biol Chem 1993;268:17126–17130.
100. Lambeth JD, Seybert DW, Kamin H. Ionic effects on adrenal steroidogenic electron transport: the role of adrenodoxin as an electron shuttle. J Biol Chem 1979;254:7255–7264.
101. Lambeth JD, Seybert DW, Kamin H. Adrenodoxin reductase-adrenodoxin complex. Rapid formation and breakdown of the complex and a slow conformational change in the flavoprotein. J Biol Chem 1980;255:4667–4672.
102. Lambeth JD, McCaslin DR, Kamin H. Adrenodoxin reductase–adrenodoxin complex: catalytic and thermodynamic properties. J Biol Chem 1976;251:7545–7550.
103. Hamamoto I, Kurokohchi K, Tanaka S, Ichikawa Y. Adrenoferredoxin-binding peptide of NADPH-adrenoferredoxin reductase. Biochim Biophys Acta 1998;953:207–213.
104. Hamamoto I, Ichikawa Y. Modification of a lysine residue of adrenodoxinreductase, essential for complex formation with adrenodoxin. Biochim Biophys Acta 1984;786:32–41.
105. Lambeth JD, Geren LM, Millett F. Adrenodoxin interaction with adrenodoxin reductase and cytochrome P-450scc. Cross-linking of protein complexes and effects of adrenodoxin modification by 1-ethyl-3-(3-dimethylaminopropyl)carbodiimide. J Biol Chem 1984;259:10025–10029.
106. Taniguchi T, Kimura T. Studies on nitrotyrosine-82 and aminoty-

rosine-82 derivatives of adrenodoxin. Effects of chemical modification on the complex formation with adrenodoxin reductase. Biochemistry 1976;15:2849–2853.
107. Cupp JR, Vickery LE. Adrenodoxin with a COOH-terminal deletion (des 116-128) exhibits enhanced activity. J Biol Chem 1989;264:1602–1607.
108. Lambeth JD, Pember SO. Cytochrome P-450scc-adrenodoxin complex. Reduction properties of the substrate-associated cytochrome and relation of the reduction states of heme and iron-sulfur centers to association of the proteins. J Biol Chem 1983;258:5596–5602.
109. Beckert V, Bernhardt R. Specific aspects of electron transfer from adrenodoxin to cytochromes P450scc and P45011beta. J Biol Chem 1997;272:4883–4888.
110. Sugano S, Morishima N, Ikeda N, Horie S. Sensitive assay of cytochrome P450scc activity by high-performance liquid chromatography. Anal Biochem 1989;182:327–333.
111. Shikita M, Hall PF. The stoichiometry of the conversion of cholesterol and hydroxycholesterols to pregnenolone (3beta-hydroxypregn-5-en-20-one) catalyzed by adrenal cytochrome P-450. Proc Natl Acad Sci USA 1974;71:1441–1445.
112. Seybert DW, Lambeth JD, Kamin H. The participation of a second molecule of adrenodoxin in cytochrome P-450-catalyzed 11beta hydroxylation. J Biol Chem 1978;253:8355–8358.
113. Takikawa O, Gomi T, Suhara K, Itagaki E, Takemori S, Katagiri M. Properties of an adrenal cytochrome P-450 ($P\text{-}450_{scc}$) for the side chain cleavage of cholesterol. Arch Biochem Biophys 1978; 190:300–306.
114. Lambeth JD, Seybert DW, Kamin H. Phospholipid vesicle-reconstituted cytochrome P-450SCC. Mutually facilitated binding of cholesterol and adrenodoxin. J Biol Chem 1980;255:138–143.
115. Lambeth JD, Kriengsiri S. Cytochrome P-450scc-adrenodoxin interactions. Ionic effects on binding, and regulation of cytochrome reduction by bound steroid substrates. J Biol Chem 1985;260:8810–8816.
116. Katagiri M, Takikawa O, Sato H, Suhara K. Formation of a cytochrome P-450scc-adrenodoxin complex. Biochem Biophys Res Commun 1977;77:804–809.
117. Hanukoglu I, Spitsberg V, Bumpus JA, Dus KM, Jefcoate CR. Adrenal mitochondrial cytochrome P-450scc. Cholesterol and adrenodoxin interactions at equilibrium and during turnover. J Biol Chem 1981;256:4321–4328.
118. Jefcoate CR. pH modulation of ligand binding to adrenal mitochondrial cytochrome P-450scc. J Biol Chem 1982;257:4731–4737.
119. Geren LM, O'Brien P, Stonehuerner J, Millett F. Identification of specific carboxylate groups on adrenodoxin that are involved in the interaction with adrenodoxin reductase. J Biol Chem 1984; 259:2155–2160
120. Coghlan VM, Vickery LE. Expression of human ferredoxin and assembly of the [2Fe-2S] center in *Escherichia coli.* Proc Natl Acad Sci USA 1989;86:835–839.
121. Palin MF, Berthiaume L, Lehoux JG, Waterman MR, Sygusch J. Direct expression of mature bovine adrenodoxin in *Escherichia coli.* Arch Biochem Biophys 1992;295:126–131.
122. Wada A, Mathew PA, Barnes HJ, Sanders D, Estabrook RW, Waterman MR. Expression of functional bovine cholesterol side chain cleavage cytochrome P450 (P450scc) in *Escherichia coli* Arch Biochem Biophys 1991;290:376–380.
123. Tuls J, Geren L, Millett F. Fluorescein isothiocyanate specifically modifies lysine 338 of cytochrome P-450scc and inhibits adrenodoxin binding. J Biol Chem 1989;264:16421–16425.
124. Tsubaki M, Iwamoto Y, Hiwatashi A, Ichikawa Y. Inhibition of electron transfer from adrenodoxin to cytochrome P-450scc by chemical modification with pyridoxal 5'-phosphate: identification of adrenodoxin-binding site of cytochrome P-450scc. Biochemistry 1989;28:6899–6907.
125. Wada A, Waterman MR. Identification by site-directed mutagenesis of two lysine residues in cholesterol side chain cleavage cytochrome P450 that are essential for adrenodoxin binding. J Biol Chem 1992;267:22877–22882.
126. Coghlan VM, Vickery LE. Electrostatic interactions stabilizing ferredoxin electron transfer complexes. J Biol Chem 1992;267: 8932–8935.
127. Miura S, Tomita S, Ichikawa Y. Modification of histidine 56 in adrenodoxin with diethyl pyrocarbonate inhibited the interaction with cytochrome P-450scc and adrenodoxin reductase. J Biol Chem 1991;266:19212–19216.
128. Cao PR, Bernhardt R. Modulation of aldosterone biosynthesis by adrenodoxin mutants with different electron transport efficiencies. Eur J Biochem 1999;265:152–159.
129. Marcus RA, Sutin N. Electron-transfers in chemistry and biology. Biochim Biophys Acta 1985;811:256–322.
130. Hintz MJ, Peterson JA. The kinetics of reduction of cytochrome P-450cam by reduced putidaredoxin. J Biol Chem 1981;256:6721–6728.
131. Benson DE, Suslick KS, Sligar SG. Reduced oxy intermediate observed in D251N cytochrome P450cam. Biochemistry 1997;36: 5104–5107.
132. Raag R, Poulos TL. Crystal structure of the carbon monoxide-substrate-cytochrome P-450CAM ternary complex. Biochemistry 1989;28:7586–7592.
133. Sligar SG, Debrunner PG, Lipscomb JD, Namtvedt MJ, Gunsalus IC. A role of the putidaredoxin COOH-terminus in P-450cam hydroxylations. Proc Natl Acad Sci USA 1974;71:3906–3910.
134. Davies MD, Sligar SG. Genetic variants in the putidaredoxin-cytochrome P-450cam electron-transfer complex: identification of the residue responsible for redox-state-dependent conformers. Biochemistry 1992;31:11383–11389.
135. Geren L, Tuls J, O'Brien P, Millett F, Peterson JA. The involvement of carboxylate groups of putidaredoxin in the reaction with putidaredoxin reductase. J Biol Chem 1986;261:15491–15495.
136. Aoki M, Ishimori K, Morishima I. Roles of negatively charged surface residues of putidaredoxin in interactions with redox partners in P450cam monooxygenase system. Biochim Biophys Acta 1998;1386:157–167.
137. Holden M, Mayhew M, Bunk D, Roitberg A, Vilker V. Probing the interactions of putidaredoxin with redox partners in camphor P450 5-monooxygenase by mutagenesis of surface residues. J Biol Chem 1997;272:21720–21725.
138. Nakamura K, Horiuchi T, Yasukochi T, Sekimizu K, Hara T, Sagara Y. Significant contribution of arginine-112 and its positive charge of *Pseudomonas putida* cytochrome P-450cam in the electron transport from putidaredoxin. Biochim Biophys Acta 1994;1207:40–48.
139. Roitberg ER, Holden MJ, Mayhew MP, Kurnikov IV, Beratan DN, Vilker VL. Binding and electron transfer between putidaredoxin and cytochrome P450cam. J Am Chem Soc 1998;120:8927–8932.
140. Lipscomb JD, Sligar SG, Namtvedt MJ, Gunsalus IC. Autooxidation and hydroxylation reactions of oxygenated cytochrome P-450cam. J Biol Chem 1976;251:1116–1124.
141. Xia B, Volkman BF, Markley JL. Evidence for oxidation-state-dependent conformational changes in human ferredoxin from multinuclear, multidimensional NMR spectroscopy. Biochemistry 1998;37:3965–3973.
142. Stout CD. Refinement of the 7 Fe ferredoxin from *Azotobacter vinelandii* at 19 Å resolution. J Mol Biol 1989;205:545–555.
143. Fukuyama K, Ueki H, Nakamura H, Tsukihara T, Matsubara H. Tertiary structure of [2Fe-2S] ferredoxin from *Spirulina platensis* refined at 25 Å resolution: structural comparisons of plant-type ferredoxins and an electrostatic potential analysis. J Biochem (Tokyo) 1995;117:1017–1023.
144. Beckert V. Bedeutung der Aminosäuren Tyrosin-82, Aspartat-76 und Histidin-56 für die strukturellen und funktionellen Eigenschaften von Adrenodoxin. PhD Thesis. Humboldt Universität, Berlin; 1999.
145. Pearson WR, Lipman DJ. Improved tools for biological sequence comparison. Proc Natl Acad Sci USA 1998;85:2444–2448.
146. Corpet F. Multiple sequence alignment with hierarchical clustering. Nucleic Acids Res 1988;16:10881–10890.
147. Nicholls A, Sharp KA, Honig B. Protein folding and association: insights from the interfacial and thermodynamic properties of hydrocarbons. Proteins 1991;11:281–296